The expression of *HOXC10* is correlated with tumor-infiltrating immune cells in basal-like breast cancer and serves as a prognostic biomarker

Xiaobei Zhang[1,2,3]^, Ying Zheng[1,2,3]^, Xiaofeng Liu[2,3,4]^, Kaiyuan Wang[1,2,3]^, Hongwei Zhao[1,2,3]^, Yiqing Yin[1,2,3]^, Yue Yu[2,3,4,5]^

[1]Department of Anesthesiology, Tianjin Medical University Cancer Institute and Hospital, National Clinical Research Center for Cancer, Tianjin, China; [2]Key Laboratory of Cancer Prevention and Therapy, Tianjin, China; [3]Tianjin's Clinical Research Center for Cancer, Tianjin, China; [4]Key Laboratory of Breast Cancer Prevention and Therapy, Tianjin Medical University, Ministry of Education, Tianjin, China; [5]The First Department of Breast Cancer, Tianjin Medical University Cancer Institute and Hospital, National Clinical Research Center of Cancer, Tianjin, China

Contributions: (I) Conception and design: Y Yu; (II) Administrative support: Y Yin; (III) Provision of study materials or patients: X Zhang, Y Zheng; (IV) Collection and assembly of data: X Zhang, X Liu; (V) Data analysis and interpretation: K Wang, H Zhao; (VI) Manuscript writing: All authors; (VII) Final approval of manuscript: All authors.

Correspondence to: Yue Yu. The First Department of Breast Cancer, Tianjin Medical University Cancer Institute and Hospital, Tianjin 300060, China. Email: yuyue@tmu.edu.cn; Yiqing Yin. Department of Anesthesiology, Tianjin Medical University Cancer Institute and Hospital, Tianjin 300060, China. Email: yyq518@sina.com.

Background: Homeobox gene C10 (*HOXC10*) plays a vital role in the occurrence and development of several cancers, but its effects and underlying mechanism in the prognosis of different subtypes of breast cancer remain unclear.

Methods: First, we evaluated and compared the expression levels of *HOXC10* cancer to normal tissues in the Oncomine and Tumor Immune Estimation Resource (TIMER) databases. Second, the correlation between *HOXC10* and the survival of patients with different types of cancer, including breast cancer, was analyzed in the PrognoScan, Gene Expression Profiling Interactive Analysis (GEPIA), and Kaplan-Meier plotter databases. Finally, the relationship between *HOXC10* and immune-infiltration levels or gene marker sets of immune cells in basal-like breast cancer (BLBC) was investigated in the TIMER and GEPIA databases.

Results: The expression of *HOXC10* was elevated in breast cancer tissues. High *HOXC10* expression indicated a poor prognosis for breast cancer patients, and expression affected the survival time of lymph-node positive or grade III breast cancer patients. In BLBC, the median overall survival (OS) of patients with high *HOXC10* expression was significantly shorter than that of patients with low *HOXC10* expression. *HOXC10* was positively correlated with the immune infiltration of macrophages in BLBC. Breast cancer patients with low *HOXC10* expression in different enriched immune-cell subgroups had a favorable prognosis.

Conclusions: The level of *HOXC10* expression increased significantly in breast cancer, and elevated *HOXC10* was positively correlated with immune-cell infiltration and poor prognosis in BLBC. These findings shed light on the important role of *HOXC10* in breast cancer. *HOXC10* should be recognized as a prognostic biomarker for determining prognosis and immune infiltration in BLBC patients.

Keywords: Homeobox gene C10 (*HOXC10*); breast cancer; basal-like breast cancer (BLBC); immune cell; immune infiltration

Submitted Nov 12, 2021. Accepted for publication Jan 11, 2022.
doi: 10.21037/atm-21-6611
View this article at: https://dx.doi.org/10.21037/atm-21-6611

^ ORCID: Xiaobei Zhang, 0000-0002-9244-5669; Ying Zheng, 0000-0002-5264-6431; Xiaofeng Liu, 0000-0003-0648-4897; Kaiyuan Wang, 0000-0002-8374-6427; Hongwei Zhao, 0000-0002-8651-0743; Yiqing Yin, 0000-0002-1130-6676; Yue Yu, 0000-0003-2053-9866.

Introduction

Breast cancer, which has the highest incidence of cancers in women and is the second leading cause of cancer-related deaths in women, is a heterogeneous disease with different biological and histological characteristics that lead to distinct prognoses and respond differently to specific therapies (1,2). Based on gene expression profiling, breast cancer can be divided into the following 5 intrinsic subtypes: normal-like, luminal A, luminal B, human epidermal growth factor receptor 2-enriched (Her-2+), and basal-like breast cancer (BLBC) (3). BLBC was so named because its gene expression profile is similar to that of basal cells (4,5). In clinical settings, the majority of BLBCs are triple-negative breast cancers, and estrogen receptor (ER), progesterone receptor (PR), and Her-2 are all negatively diagnosed by immunohistochemistry (6). As the most aggressive subtype of breast cancer, BLBC is characterized by early distant metastasis, a high resistant rate, and poor outcomes which comprises 8% to 20% of all breast cancer (7,8). However, as the molecular mechanisms underlying the aggressive characteristics of BLBC are not well understood, identifying new biomarkers for predicting patients' prognoses and providing targets for effective targeted therapies remain challenging. BLBC has been classified as basal-like immune activated (BLIA), basal-like immune-suppressed (BLIS), luminal androgen receptor (LAR) and mesenchymal (MES), suggesting potential immune therapeutic targets for BLBC. Thus, it is necessary to clarify the relationship between BLBC and immune invasion, and find an immune related biomarker to indicate the prognosis of BLBC.

Homeobox genes (*HOXs)* make important contributions to cell differentiation and morphogenesis in multicellular organisms by encoding a family of evolutionarily conserved transcription factors that bind to the promoters of target genes (9). In mammals, 39-gene *HOX* clusters reside in 4 separate chromosomal linkage groups designated as homeobox gene A (*HOXA*), homeobox gene B (*HOXB*), homeobox gene C (*HOXC*), and homeobox gene D (*HOXD*) that share identical organization (10). It is confirmed that *HOX* genes act as oncogenes or tumor suppressors in the occurrence and progression of many different cancers (11-14). *HOXC* genes are located on chromosome 12q13.3 (15).

Homeobox gene C10 (*HOXC10*), a member of the HOXC clusters, participates in the assembly of replicative complexes, the development of the spinal cord, and the formation of neurons by encoding a transcription factor containing a highly conserved DNA binding homeodomain (16-18). There is increasing evidence that *HOXC10* plays a vital role in the occurrence and development of several cancers by influencing cancer cell proliferation, apoptosis, invasion and avoidance of immune destruction (19-21). Zhai *et al.* (22) analyzed normal cervical epithelial tissue, cervical intraepithelial neoplasia, and invasive squamous cell carcinoma tissues by gene chip and found that *HOXC10* expression was upregulated with the increase of cervical epithelial malignancy, which confirmed that HOXC10 protein was related to the progression of cervical cancer *in vivo* and *in vitro*. Researchers have also found that the high expression of HOXC10 protein is closely related to the poor prognosis of thyroid cancer (23). In breast cancer research, it has been shown that *HOXC10* is highly expressed in breast cancer and also an estrogen-responsive gene which might be associated with hormone-induced cell differentiation, development and human diseases (18). However, the effects and mechanisms underlying *HOXC10* in the prognoses of different subtypes of breast cancer, especially BLBC, remain unclear.

In the present study, the different expression levels of *HOXC10* in different cancer and normal tissues were assessed by the Oncomine and Tumor Immune Estimation Resource (TIMER) databases. The correlations between *HOXC10* and the prognoses of cancer patients, including those with different subtypes of breast cancer, were analyzed using the PrognoScan, Gene Expression Profiling Interactive Analysis (GEPIA) and Kaplan-Meier plotter databases. Further, the relationship between *HOXC10* and the immune-infiltration levels of immune cells in different tumor microenvironments were investigated in the TIMER database. The findings of this study shed light on the predictive role of *HOXC10* in the prognoses of patients with BLBC and also identify a potential mechanism related to immune infiltration.

We present the following article in accordance with the REMARK reporting checklist (available at https://atm.amegroups.com/article/view/10.21037/atm-21-6611/rc).

Methods

Analysis in the Oncomine database

The *HOXC10* expression of various types of cancers was identified in the Oncomine database (https://www.oncomine.org/resource/login.html) (24). The threshold was determined according to the following values: a P value of 0.001, a fold change of 1.5, and the gene ranking

of all. The data came from messenger ribonucleic acid (mRNA).

Survival analyses in the PrognoScan, GEPIA, and Kaplan-Meier plotter databases

To investigate the effects of *HOXC10* in the prognosis of different types of cancer, the correlations between *HOXC10* expression levels and the survival of cancer patients were analyzed using the PrognoScan (http://www.abren.net/PrognoScan/) (25), GEPIA (http://gepia.cancer-pku.cn/index.html) (26), and Kaplan-Meier plotter databases (http://kmplot.com/analysis/) (27). The Kaplan-Meier plotter database were analyzed by filtering the intrinsic subtypes of breast cancer including BLBC to evaluate the relationship between *HOXC10* expression and the outcomes of breast cancer patients with different intrinsic subtypes. The threshold was determined according to the following values: a Cox P value <0.05 in the PrognoScan database, and a log-rank P value <0.05 in the GEPIA and Kaplan-Meier plotter databases. The study was conducted in accordance with the Declaration of Helsinki (as revised in 2013).

Correlation analyses between HOXC10 and immune cells in the TIMER, GEPIA, and Kaplan-Meier plotter databases

To systematically analyze the levels of immune invasion in diverse types of cancers and differences in the gene expression of different cancers, we used the TIMER database (https://cistrome.shinyapps.io/timer/) to evaluate data from The Cancer Genome Atlas (TCGA), which included 10,897 samples across 32 cancer types (28,29). First, we confirmed the expression of *HOXC10* across data from 32 cancer tissues compared to data from paired normal tissues using the TIMER database. Second, we investigated the correlations of *HOXC10* with typical infiltrating immune cells [i.e., B cells, cluster of differentiation (CD)4$^+$ T cells, CD8$^+$ T cells, neutrophils, macrophages, and dendritic cells (DCs)] using the TIMER algorithm. Third, we further analyzed the correlations between *HOXC10* and genetic markers of immune cells in breast invasive carcinoma (BRCA) and different intrinsic subtypes of BRCA via correlation modules in the TIMER database. The gene markers of tumor-infiltrating immune cells included the markers of B cells, CD8$^+$ T cells, general T cells, neutrophils, natural killer (NK) cells, monocytes, tumor-associated macrophages (TAMs), M1 macrophages, M2 macrophages, DCs, T-helper 1 (Th1) cells, T-helper (Th2) cells, follicular helper T (Tfh) cells, Th17 cells, regulatory cells (Tregs), and T cell exhaustion as described in previous studies (30,31).

The comprehensive GEPIA database, which comprises 9,736 tumor samples and 8,587 normal samples from TCGA and the Genotype-Tissue Expression Project (GTEx) programs (26), was also used to further confirm the significantly correlated genes in TIMER, which analyzes RNA-sequencing expression. The Spearman's correlation test was selected, and all other default settings were accepted before analyzing the gene correlations.

Finally, to confirm the correlations between *HOXC10* and biomarkers of immune cells in BRCA, we used a pan-cancer analysis of the Kaplan-Meier plotter database to export the different outcomes of patients with BRCA based on different levels of immune cells. The automatic best performing threshold was used as the cutoff. The results displayed the false discovery rates in addition to the P values.

Statistical analysis

The results of the Oncomine analysis are displayed with their P values, fold changes, and ranks. The survival curves were generated by the PrognoScan, GEPIA, and Kaplan-Meier plotter databases, and were displayed with the hazard ratio (HR) and P or Cox P values from the log-rank tests. The Spearman's correlation analysis and statistical significance results were used to evaluate correlations between *HOXC10* and immune infiltration or type markers of immune cells. For all the analyses in the present study, a P value <0.05 was considered statistically significant.

Results

The mRNA expression levels of HOXC10 in different human cancers

To study changes in *HOXC10* expression between normal and tumor tissues, the *HOXC10* mRNA levels of different tumors and normal tissues of multiple cancer types were analyzed first using the Oncomine database, from which 147 data sets were selected, including 30,079 samples. The analysis showed that the expression levels of *HOXC10* were significantly higher in brain and central nervous system (CNS), breast, cervical, colorectal, esophageal, gastric, lung and sarcoma cancers tissues than normal tissues (see

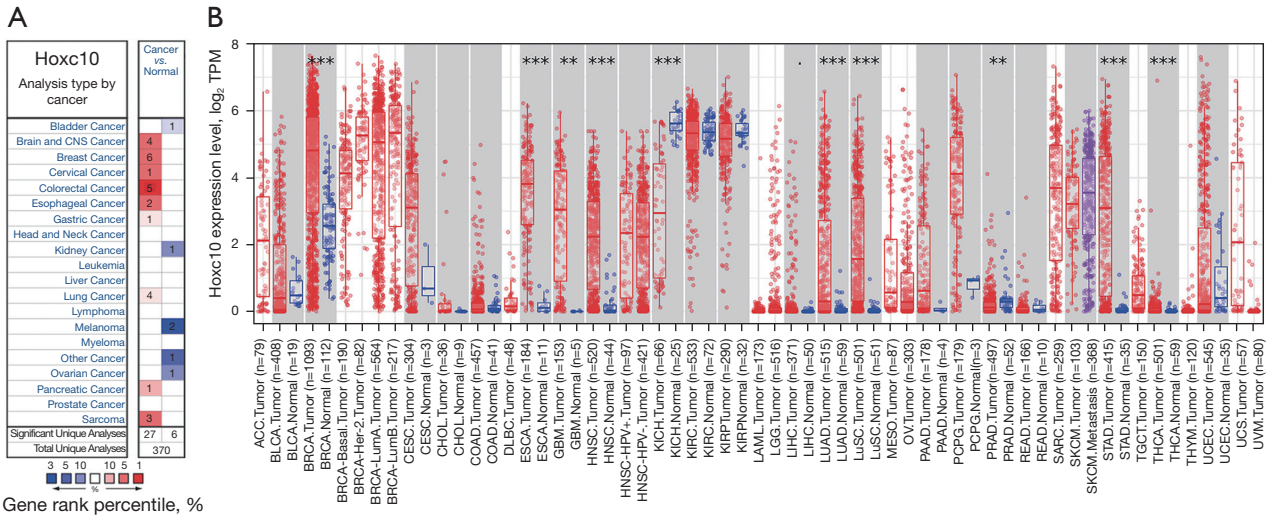

Figure 1 The mRNA expression levels of *HOXC10* in different types of cancer. (A) The differential expression level of *HOXC10* in different cancer and normal tissues in the Oncomine database. (The threshold was determined according to the following values: a P value of 0.001, a fold change of 1.5, and the gene ranking of all); (B) *HOXC10* expression levels of different tumor types in TCGA database were detected by TIMER, and were significantly higher in the BRCA, ESCA, GBM, HNSC, LUAD, LUSC, STAD, and THCA tissues than the adjacent normal tissues. **, P<0.01; ***, P<0.001. HOXC10, Homeobox gene C10; TCGA, The Cancer Genome Atlas; TIMER, Tumor Immune Estimation Resource; BRCA, breast invasive carcinoma; ESCA, esophageal carcinoma; GBM, glioblastoma multiforme; HNSC, head and neck squamous cell carcinoma; LUAD, lung adenocarcinoma; LUSC, lung squamous cell carcinoma; STAD, stomach adenocarcinoma; THCA, thyroid carcinoma.

Figure 1A). Additionally, the expression levels of *HOXC10* were lower in kidney, melanoma, and ovarian cancer tissues than normal tissues in some data sets. The detailed results of *HOXC10* expression in different cancer types are summarized in Table S1.

To further evaluate *HOXC10* expression in human cancers, we analyzed the expression levels of *HOXC10* between different tumor and normal tissues based on the RNA-sequencing data of multiple malignancies in TCGA database. *Figure 1B* shows the differential expression of *HOXC10* between the tumor and adjacent normal tissues across all TCGA tumors. The expression levels were significantly higher in BRCA, esophageal carcinoma (ESCA), glioblastoma multiforme (GBM), head and neck squamous cell carcinoma (HNSC), lung adenocarcinoma (LUAD), lung squamous cell carcinoma (LUSC), stomach adenocarcinoma (STAD), and thyroid carcinoma (THCA) tissues than adjacent normal tissues. However, *HOXC10* expression was significantly lower in kidney chromophobe (KICH) and prostate adenocarcinoma (PRAD) tissues than adjacent normal tissues (see *Figure 1B*).

Predictive effect of HOXC10 in the prognosis of patients with different cancers

Based on the differences in *HOXC10* expression between tumor and normal tissues, we first analyzed the associations between *HOXC10* and survival across different cancers using the PrognoScan database (see Table S2). Only Cox P values <0.05 are shown in *Figure 2A*. *HOXC10* expression significantly affected the prognosis of 3 type cancers (i.e., breast, brain and ovarian cancer). GSE1378 and GSE1379, 2 cohorts of 60 patients with breast cancer, respectively, indicated that a high level of *HOXC10* expression was significantly associated with a high risk of relapse in breast cancer patient [GSE1378, relapse-free survival (RFS) HR =1.27%, 95% confidence interval (CI): 1.03–1.56, Cox P=0.024856; GSE1379, RFS HR =1.25%, 95% CI: 1.01–1.54, Cox P=0.036064; see *Figure 2B,2C*]. Further, the high expression of *HOXC10* in ovarian cancer and brain cancer was related to a poor prognosis (see *Figure 2D-2F*).

Second, we used GEPIA database to analyze TCGA data to evaluate the predictive value of *HOXC10* in human cancers. Notably, the high or low expression of *HOXC10*

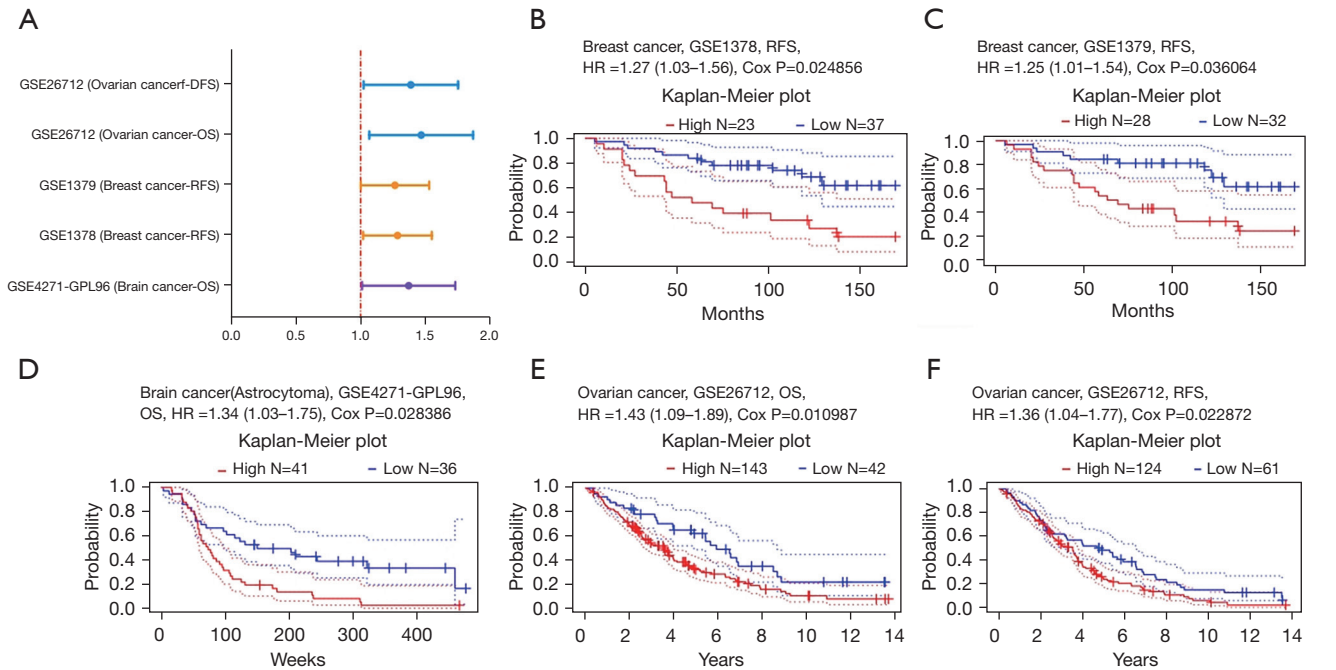

Figure 2 Prognostic potential of *HOXC10* across different cancers in the PrognoScan databases. (A) A forest plot displaying the prognostic role of *HOXC10* using the PrognoScan database (Cox P value <0.05). Orange represents the results for breast cancer; blue represents the results for ovarian cancer and purple represents the results for brain cancer; (B-F) the Kaplan-Meier survival curves between the high and low expression of *HOXC10* in different types of cancer in PrognoScan. (B,C) The Kaplan-Meier survival curves of RFS in 2 breast cancer cohorts (GSE1378, n=60; GSE1379, n=60); (D) the Kaplan-Meier survival curve of OS in a brain cancer cohort (GSE4271-GPL96, n=77); (E,F) the Kaplan-Meier survival curves for OS and DFS in an ovarian cancer cohort (GSE26712, n=185). RFS, relapse-free survival; OS, overall survival.

made no significant difference in the disease-free survival (DFS) of BRCA patients. However, BRCA patients with a low expression of *HOXC10* had better overall survival (OS) than those with a high expression of *HOXC10* (see Figure S1A). In addition, a high expression of *HOXC10* in adrenocortical carcinoma (ACC), colon adenocarcinoma (COAD), and stomach adenocarcinoma (STAD) was correlated to poor DFS and OS (see Figure S1B-D). However, the high expression of *HOXC10* in kidney renal clear cell carcinoma (KIRC) indicated a favorable prognosis (see Figure S1E).

Third, we analyzed large databases, including the Gene Expression Omnibus (GEO), European Genome-Phenome Archive (EGA), and TCGA databases, using the Kaplan-Meier plotter database to explore the potential prognostic relationship between *HOXC10* and different cancers (see Figure S2). In breast cancer, the median OS and post-progression survival (PPS) times of patients with lower levels of *HOXC10* expression were 120 and 43.2 months, respectively, while that of patients with higher levels of *HOXC10* expression were 85.2 and 26.8 months, respectively, and the differences were significant (P=0.00353 and P=0.03, respectively; see Figure S2A). The same phenomenon was observed in lung cancer and gastric cancer (see Figure S2C,D). Conversely, a higher expression of *HOCX10* was related to better RFS in ovarian cancer patients (P=0.038; see Figure S2B).

Prognostic potential of HOXC10 in BLBC

The above-mentioned 3 analyses confirmed that the expression level of *HOXC10* could be used to predict the prognosis of patients with breast cancer. To further evaluate the relationship between *HOXC10* expression and the outcomes of breast cancer patients with different intrinsic subtypes, the Kaplan-Meier plotter database was

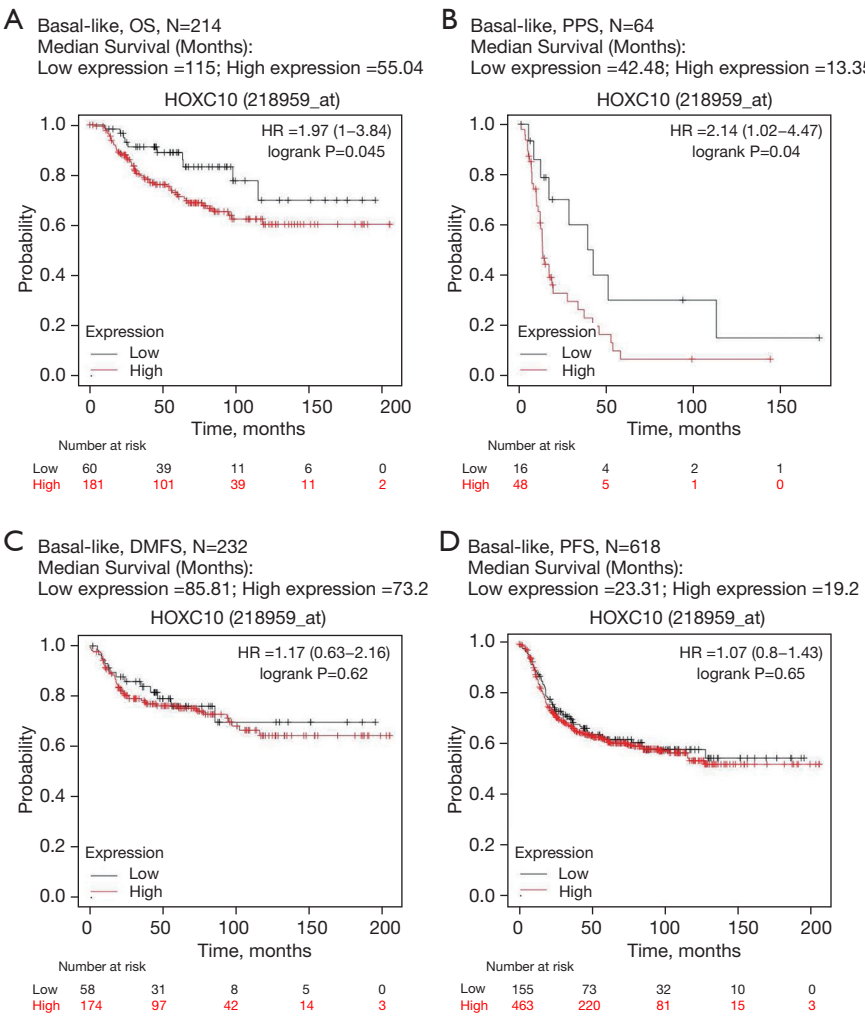

Figure 3 The expression of *HOXC10* affected the outcomes of patients with BLBC in the Kaplan-Meier plotter database. (A) OS curve (n=241); (B) PPS survival curve (n=64); (C) DMFS survival curve (n=232); (D) RFS survival curve (n=618). The OS and PPS of *HOXC10* patients in the over-expression group with BLBC were significantly longer than those of patients in the under-expression group (P=0.045 and P=0.04, respectively). BLBC, basal-like breast cancer; OS, overall survival; PPS, post-progression survival; DMFS, distant metastasis-free survival; RFS, relapse-free survival.

analyzed by filtering the intrinsic subtype of breast cancer. There was no significant difference between patients with high *HOXC10* expression and those with low *HOXC10* expression in luminal A, luminal B, and Her-2 + breast cancer (see Figure S3). Notably, the median OS of patients with high and low *HOXC10* expression in BLBC was 55.4 and 115 months, respectively, and the difference was significant (HR =1.97%, 95% CI: 1–3.87; P=0.045; see *Figure 3A*). The same prognostic effect of *HOXC10* was also found in relation to the PPS of BLBC patients (HR =2.14%, 95% CI: 1.02–4.47; P=0.04; see *Figure 3B*). There is no significant difference in RFS and DMFS (See *Figure 3C,3D*). The analysis results showed that the increased expression of *HOXC10* in BLBC was related to a poor prognosis, which indicates that *HOXC10* can serve as a biomarker for the prognosis of BLBC patients.

HOXC10 expression affects the survival time of lymph-node positive or grade III breast cancer patients

In addition to the different intrinsic subtypes that could affect the prognosis, many clinicopathological factors are

Table 1 The associations between *HOXC10* mRNA expression and the outcomes of breast cancer patients with different clinicopathological characteristics using the Kaplan-Meier plotter database

Clinicopathological characteristics	Overall survival (n=1,402)			Progression-free survival (n=3,955)		
	N	Hazard ratio	P value	N	Hazard ratio	P value
ER status						
ER positive	548	1.06 (0.71–1.58)	0.7903	2061	1.03 (0.85–1.25)	0.7426
ER negative	251	1.31 (0.77–2.23)	0.3143	801	1.17 (0.9–1.52)	0.2398
PR status						
PR positive	83	0.61 (0.15–2.46)	0.4857	589	1.02 (0.69–1.51)	0.9309
PR negative	89	0.86 (0.31–2.42)	0.7761	549	1.32 (0.93–1.87)	0.121
Her-2 status						
Her-2 positive	129	0.79 (0.38–1.64)	0.5245	252	0.9 (0.55–1.45)	0.6581
Her-2 negative	130	0.78 (0.31–1.94)	0.5876	800	1.17 (0.86–1.6)	0.3078
Lymph-node status						
LN positive	313	1.79 (1.09–2.94)	0.0206	1133	1.39 (1.09–1.77)	0.0072
LN negative	594	0.89 (0.59–1.34)	0.5738	2020	1.06 (0.87–1.29)	0.5466
Grade						
I	161	0.61 (0.23–1.58)	0.3049	345	1 (0.55–1.83)	0.99
II	387	1.05 (0.64–1.7)	0.85	901	1.13 (0.85–1.5)	0.4049
III	503	1.55 (1.03–2.33)	0.034	903	1.19 (0.92–1.54)	0.1792
TP53 status						
Mutated	111	1.5 (0.57–3.97)	0.4106	188	1.72 (0.92–3.2)	0.0851
Wild type	187	0.65 (0.32–1.29)	0.2102	273	1.09 (0.66–1.79)	0.7383

ER, estrogen receptor; PR, progesterone receptor; Her-2, human epidermal growth factor receptor 2; LN, lymph node; TP53, tumor protein p53.

related to the survival of patients with breast cancer. We used the Kaplan-Meier plotter database to examine the relationships between *HOXC10* and the prognosis of breast cancer with different clinicopathological characteristics (see *Table 1*). Notably, the elevated expression of *HOXC10* had adverse effects on both the OS and PPS of lymph-node positive breast cancer patients (OS: HR =1.79%, 95% CI: 1.09–2.94; P=0.0206; PPS: HR =1.39%, 95% CI: 1.09–1.77; P=0.0072). Moreover, high *HOXC10* expression negatively affected the OS of grade III breast cancer patients (HR =1.55%, 95% CI: 1.03–2.33; P=0.0034). Thus, *HOXC10* appears to affect the prognosis of lymph-node positive or advanced-stage (i.e., grade III) breast cancer patients.

The transcription of HOXC10 is correlated with the immune-infiltration level and immune marker set in BLBC

Tumor-infiltrating lymphocytes are independent predictors of the sentinel lymph-node status and survival of cancer patients (31). Previous research has shown that tumor infiltration is related to the prognosis of breast cancer patients (32-34). The effect of *HOXC10* transcription on the recruitment of immune cells and the cancer microenvironment remains unclear. Thus, we investigated the relationship between the immune-infiltration and transcription levels of *HOXC10* in different types of cancer (see Figure S4), including different subtypes of breast cancer

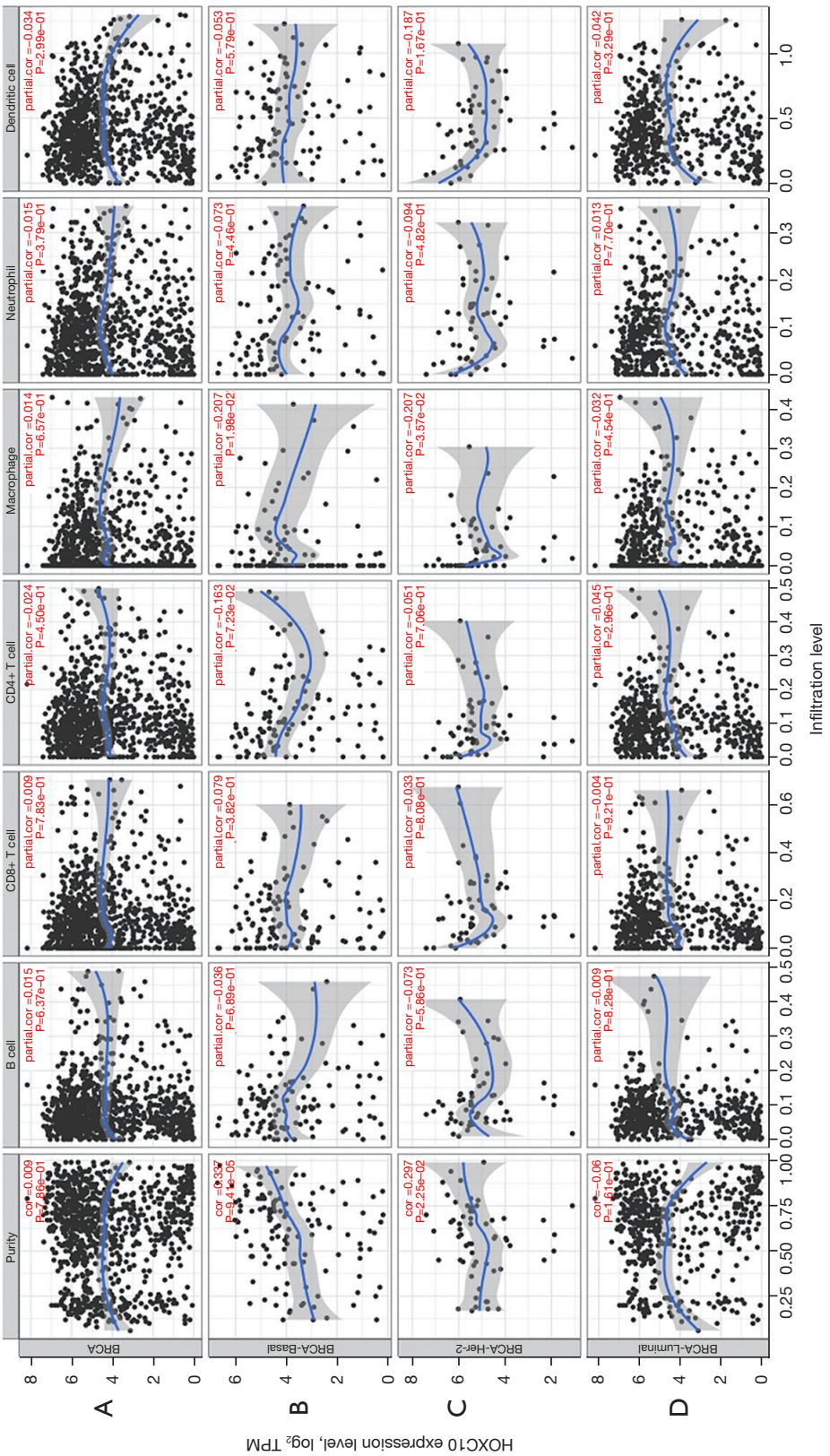

Figure 4 Correlated relationship between immune infiltration and *HOXC10* expression in different subtypes of breast cancer using the TIMER database. (A) BRCA; (B) BLBC; (C) Her-2+ breast cancer; and (D) luminal breast cancer. TIMER, Tumor Immune Estimation Resource; BRCA, breast invasive carcinoma; BLBC, basal-like breast cancer; Her-2, human epidermal growth factor receptor 2.

(see *Figure 4*) using the TIMER database to understand the mechanism underlying *HOXC10* and the outcomes of breast cancer patients. There were no significant correlations between immune-infiltration of B cells, $CD8^+$ T cells, $CD4^+$ T cells, macrophages, neutrophils, DCs and transcription levels of *HOXC10* in BRCA (see *Figure 4A*) and luminal breast cancer (see *Figure 4D*). However, *HOXC10* was positively correlated with the immune infiltration of macrophages in BLBC (Cor =0.207; P=0.0198; see *Figure 4B*), but was negatively correlated with the immune infiltration of macrophages in Her-2+ breast cancer (Cor = –0.276; P=0.0357; see *Figure 4C*).

Further, the relationships between *HOXC10* expression levels and the genetic markers of different immune cells, including B cells, $CD8^+$ T cells, general T cells, neutrophils, NK cells, monocytes, TAMs, M1 macrophages, M2 macrophages, DCs, Th1 cells, Th2 cells, Tfh cells, Th17 cells, Treg, and T cell exhaustion in BRCA were explored using the TIMER database, which showed that there were no significant correlations between *HOXC10* and these biomarkers (see *Figure 5* and *Table 2*). Next, the GEPIA database was used to explore the relationship between the biomarkers of monocytes, TAMs, M1 and M2 macrophage and *HOXC10* expression in BRCA (see Figure S5). The results showed that the *CD86*, macrophage-colony stimulating factor 1 receptor (*CSF1R*) of monocytes, the chemokine (C-C motif) ligand 2 (*CCL2*) of TAMs, the *CD163*, v-set and immunoglobulin domain–containing 4 (*VSIG4*), and membrane spanning 4-domains A4A (*MS4A4A*) of M2 macrophages were negatively correlated with *HOXC10* expression in BRCA.

Further, we explored the correlations between *HOXC10* and genetic markers in different subtypes of BRCA. As *Figure 5* shows, in contrast to its positive correlation with *HOXC10* expression in luminal breast cancer, the correlations between genetic markers of immune cells in BLBC and Her-2+ were mostly negative (see *Table 2* and Table S3). Specifically, after the correlation adjustment by purity, the complement C3a receptor 1 (*C3AR1*), *CD86* and *CSF1R* of monocytes, the *CD68* and *IL10* of TAMs, the *CD163*, *VSIG4* and *MS4A4A* of M2 macrophage, and the interferon regulatory factor 5 (*IRF5*) of M1 macrophages were found to be significantly correlated with the expression levels of *HOXC10* in BLBC (see *Table 2*). Thus, *HOXC10* appears to be closely related to macrophage polarization in BLBC, which further confirms that expressions in BLBC are correlated to immune infiltration.

Prognostic effect of HOXC10 expressions in BRCA based on immune cells

Both the TIMER and GEPIA databases were used to analyze the relationship between *HOXC10* and biomarkers of immune cells in BRCA, but the results differed. To confirm the correlation, we used the Kaplan-Meier plotter database to analyze the relationship between *HOXC10* and the OS of patients with BRCA based on different levels of immune cells. The results showed that high *HOXC10* expressions of BRCA in enriched $CD4^+$ memory T cells (HR =1.6, P=0.024), enriched macrophages (HR =1.71, P=0.034), enriched NK cells (HR =2.07, P=0.032), and enriched Th2 cells (HR =1.83, P=0.029) was negatively correlated with OS time, while the high expression of *HOXC10* had no significant correlation with OS in decreased subgroups of the immune-cells (see *Figure 6*). There was no significant correlation between high *HOXC10* and the outcomes of BRCA patients with enriched B cells, regulatory T cells, and Th1 cells. However, compared to the low *HOXC10* expression group, the high *HOXC10* expression group had a poorer prognosis regardless of whether or not they had enriched or decreased $CD8^+$ memory T cells, eosinophils, and MES stem cells (see Figure S6). We also analyzed the prognostic potential of RFS in BRCA based on the different immune-cell subgroup (see Figure S7). All the results indicated that a high level of *HOXC10* affects the survival of BRCA patients, which may be due to the infiltration of some immune cells.

Discussion

HOXC10, which is known to regulate the rib formation of mammals (35,36), is a key regulator in the development, proliferation, invasion, and metastasis of cancer cells in lung cancer (19), glioma (20), gastric cancer (37), thyroid cancer (23), and squamous cell carcinomas (22). In the present study, we examined the abnormal expression and predictive effect of *HOXC10* in different types of cancers, especially in different subtypes of breast cancer. We also evaluated the correlations between *HOCX10* and cancer immune infiltrates to clarify whether *HOXC10* affected the prognosis of breast cancer patients.

To examine the effects of *HOXC10* on different types of cancer, we used 2 independent online databases (i.e., Oncomine and TIMER) to analyze the differential expression of *HOXC10* in tumor and adjacent normal tissues. The Oncomine analysis showed that the expression levels

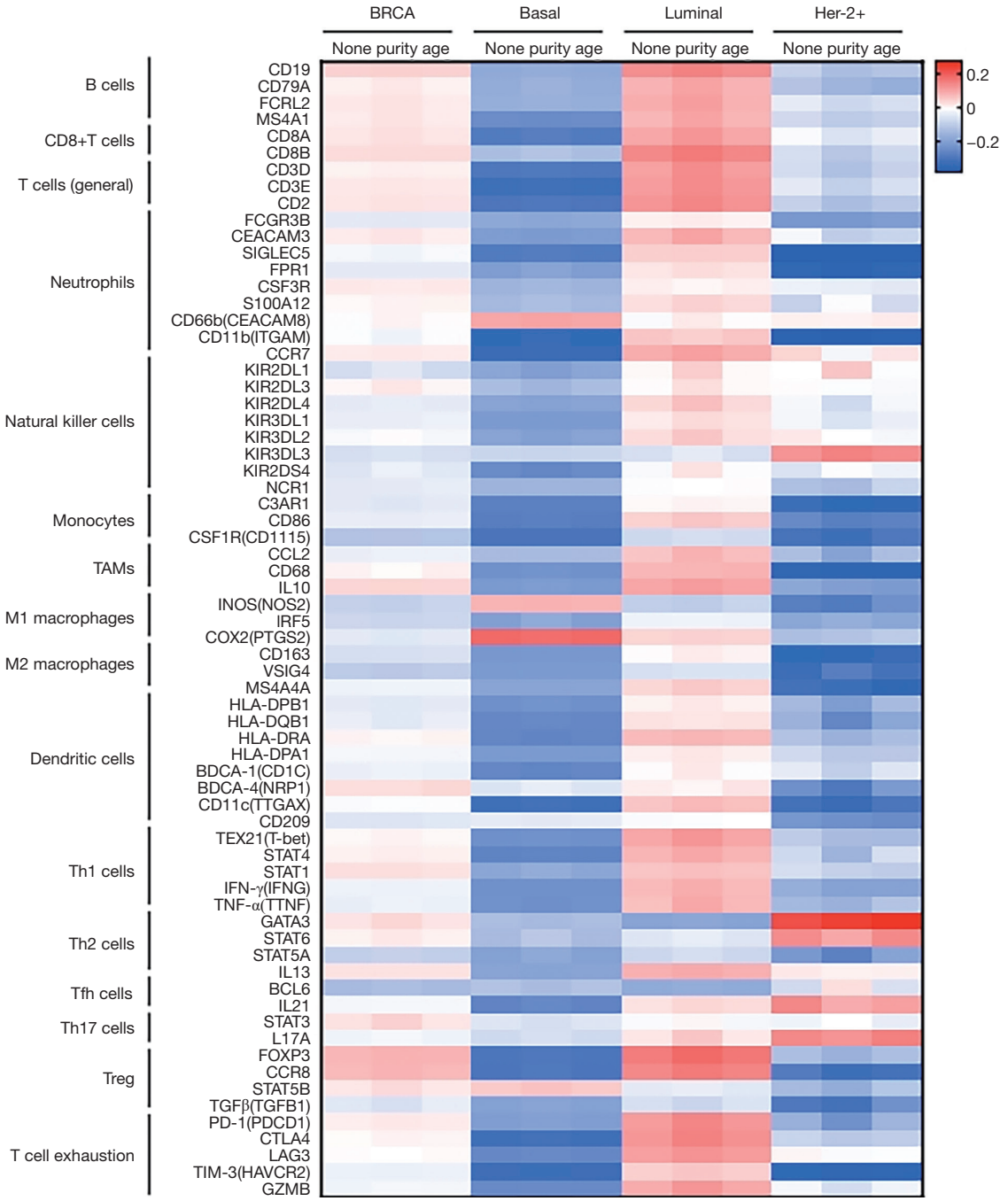

Figure 5 The heatmap of the correlations between *HOXC10* and the genetic markers of the infiltrating immune cells (including B cells, $CD8^+$ T cells, general T cells, neutrophils, NK cells, Monocytes, TAMs, M1 macrophages, M2 macrophages, DCs, Th1 cells, Th2 cells, Tfh cells, Th17 cells, Treg, and T cell exhaustion) detected by the TIMER database in BRCA and different intrinsic subtypes of BRCA. CD, cluster of differentiation; NK, natural killer; TAM, tumor-associated macrophage; DC, dendritic cell; Th, T-helper; Tfh, follicular helper T; Treg, regulatory cells; TIMER, Tumor Immune Estimation Resource; BRCA, breast invasive carcinoma.

Table 2 Correlations between *HOXC10* and the genetic markers of infiltrating immune cells in breast cancer and BLBC patients

Description	Gene markers	Breast cancer				BLBC			
		None		Purity		None		Purity	
		COR	P	COR	P	COR	P	COR	P
B cells	*CD19*	0.0465	0.12308	0.0503	0.11279	–0.172	0.04211	–0.1652	0.06136
	CD79A	0.0138	0.64678	0.0227	0.47361	–0.1649	0.05163	–0.1511	0.08733
	FCRL2	0.0207	0.49323	0.0292	0.35728	–0.161	0.05743	–0.1554	0.07873
	MS4A1	0.0188	0.53424	0.0286	0.36739	–0.2399	0.0043	–0.2414	0.00585
$CD8^+$ T cells	*CD8A*	0.0242	0.42181	0.0309	0.33097	–0.2799	0.00085	–0.2709	0.00196
	CD8B	0.0363	0.22867	0.0387	0.22265	–0.1258	0.13842	–0.1072	0.22644
T cells (general)	*CD3D*	0.0117	0.69912	0.016	0.61489	–0.2878	0.00059	–0.2829	0.00121
	CD3E	0.021	0.48641	0.0258	0.41581	–0.3114	0.00019	–0.3066	0.00043
	CD2	0.0252	0.40456	0.0291	0.35933	–0.2909	0.00051	–0.2858	0.00107
Neutrophils	*FCGR3B*	–0.034	0.26644	–0.0377	0.23494	–0.1739	0.03987	–0.1804	0.04076
	CEACAM3	0.0183	0.54328	0.026	0.41242	–0.2023	0.01651	–0.2066	0.01885
	SIGLEC5	–0.012	0.6846	–0.0172	0.5872	–0.2804	0.00083	–0.2746	0.00169
	FPR1	–0.036	0.23721	–0.0355	0.26384	–0.2003	0.01777	–0.1853	0.03568
	CSF3R	0.0216	0.47348	0.0183	0.56378	–0.1501	0.07673	–0.1374	0.12035
	S100A12	0.0048	0.87368	0.0098	0.75699	–0.1344	0.11347	–0.12	0.17561
	CEACAM8	–0.005	0.86922	0.0104	0.7435	0.1001	0.23947	0.10664	0.22904
	ITGAM	–0.007	0.82108	–0.0196	0.53738	–0.3327	6.49E–05	–0.3285	0.00016
	CCR7	0.0193	0.52247	0.0213	0.50218	–0.3262	9.14E–05	–0.3249	0.00019
Natural killer cells	*KIR2DL1*	–0.061	0.04302	–0.0382	0.22844	–0.1815	0.03183	–0.1982	0.02435
	KIR2DL3	0.0073	0.8086	0.024	0.44993	–0.125	0.14118	–0.1431	0.10572
	KIR2DL4	–0.035	0.24025	–0.0307	0.33266	–0.1852	0.02849	–0.1901	0.03092
	KIR3DL1	–0.027	0.37454	–0.0272	0.39137	–0.2063	0.01448	–0.2099	0.01696
	KIR3DL2	–0.01	0.74839	0.0031	0.92324	–0.1862	0.02758	–0.1939	0.0277
	KIR3DL3	–0.057	0.00702	–0.0469	0.0364	–0.0763	0.20286	–0.0786	0.2083
	KIR2DS4	–0.044	0.14704	–0.0237	0.45493	–0.2407	0.00417	–0.2528	0.00385
	NCR1	–0.038	0.20267	–0.0369	0.24511	–0.1494	0.07804	–0.1478	0.09458
Monocytes	*C3AR1*	–0.039	0.19612	–0.0422	0.18389	–0.2644	0.00165	–0.2638	0.0026
	CD86	–0.028	0.34912	–0.0299	0.34683	–0.2717	0.00121	–0.2669	0.0023
	CSF1R	–0.112	0.00021	–0.1096	0.0005	–0.2974	0.00038	–0.2959	0.0007
TAMs	*CCL2*	–0.027	0.36706	–0.0231	0.46604	–0.1282	0.13095	–0.1297	0.14264
	CD68	0.0105	0.72878	0.0033	0.91686	–0.2297	0.00643	–0.2253	0.01038
	IL10	0.0428	0.15599	0.0439	0.16637	–0.2085	0.01357	–0.2019	0.0219

Table 2 (*continued*)

Table 2 (*continued*)

Description	Gene markers	Breast cancer				BLBC			
		None		Purity		None		Purity	
		COR	P	COR	P	COR	P	COR	P
M1 macrophages	*NOS2*	–0.084	0.00551	–0.0871	0.006	0.0824	0.33338	0.0881	0.32081
	IRF5	–0.072	0.01708	–0.0742	0.0192	–0.1965	0.02011	–0.1702	0.05396
	PTGS2	–0.038	0.21377	–0.041	0.196	0.1884	0.02594	0.18034	0.04097
M2 macrophages	*CD163*	–0.058	0.05648	–0.0558	0.07849	–0.2163	0.0104	–0.2144	0.01482
	VSIG4	–0.097	0.00123	–0.0978	0.002	–0.2077	0.01395	–0.2056	0.01959
	MS4A4A	–0.019	0.5244	–0.0183	0.56427	–0.1845	0.02926	–0.1854	0.0356
Dendritic cells	*HLA–DPB1*	–0.037	0.2167	–0.0404	0.20339	–0.2307	0.00621	–0.2245	0.01067
	HLA–DQB1	–0.025	0.41401	–0.0405	0.20181	–0.2494	0.00304	–0.2451	0.00521
	HLA–DRA	0.0105	0.72911	0.0062	0.84426	–0.2521	0.00273	–0.2544	0.00372
	HLA–DPA1	–0.015	0.62853	–0.016	0.61391	–0.2102	0.0128	–0.2063	0.01914
	CD1C	–0.025	0.40064	–0.0197	0.53471	–0.2507	0.00282	–0.2557	0.00345
	NRP1	0.0331	0.27264	0.0326	0.30492	–0.0458	0.59081	–0.0313	0.7245
	ITGAX	–0.009	0.76693	–0.0067	0.83264	–0.3097	0.00021	–0.3043	0.00048
	CD209	–0.043	0.1503	–0.0448	0.15788	–0.0325	0.70262	–0.038	0.66897
Th1 cells	*TBX21*	0.0062	0.83834	0.0108	0.73436	–0.2319	0.00593	–0.2268	0.00987
	STAT4	0.0121	0.68963	0.0168	0.59651	–0.2586	0.0021	–0.2569	0.00338
	STAT1	0.0311	0.302	0.0318	0.31629	–0.1806	0.03288	–0.1666	0.05929
	IFNG	–0.019	0.51824	–0.0212	0.50352	–0.228	0.00674	–0.229	0.00903
	TNF	–0.03	0.31225	–0.0202	0.52431	–0.227	0.0071	–0.2341	0.0077
Th2 cells	*GATA3*	0.0266	0.37862	0.0412	0.19378	–0.1227	0.14842	–0.1324	0.13453
	STAT6	0.0116	0.70183	0.0208	0.51217	–0.1279	0.1319	–0.0999	0.25956
	STAT5A	–0.09	0.00288	–0.0804	0.0112	–0.1911	0.02387	–0.1723	0.05092
	IL13	0.0287	0.342	0.0292	0.35764	–0.1848	0.0288	–0.1868	0.03401
Tfh cells	*BCL6*	–0.131	1.26E–05	–0.12	0.0001	–0.1123	0.18628	–0.1259	0.15487
	IL21	–0.015	0.61721	–0.0136	0.66722	–0.2584	0.00206	–0.2468	0.00481
Th17 cells	*STAT3*	0.0293	0.33211	0.0473	0.13584	–0.0419	0.62252	–0.0566	0.52339
	IL17A	–0.017	0.56991	–0.0114	0.71881	–0.0662	0.43707	–0.0541	0.5426
Tregs	*FOXP3*	0.0801	0.00785	0.0874	0.0058	–0.2933	0.00046	–0.2842	0.00114
	CCR8	0.0756	0.01218	0.085	0.0073	–0.2948	0.00041	–0.2825	0.00118
	STAT5B	0.0232	0.44267	0.0398	0.20948	0.0554	0.51494	0.06682	0.45131
	TGFB1	–0.04	0.18603	–0.0551	0.08212	–0.1915	0.02354	–0.1844	0.03652

Table 2 (*continued*)

Table 2 (*continued*)

Description	Gene markers	Breast cancer				BLBC			
		None		Purity		None		Purity	
		COR	P	COR	P	COR	P	COR	P
T-cell exhaustion	*PDCD1*	0.016	0.59556	0.0218	0.49221	–0.2002	0.01772	–0.1935	0.028
	CTLA4	0.0043	0.88702	0.0106	0.73839	–0.3091	0.00022	–0.3061	0.00044
	LAG3	0.0032	0.91633	–0.001	0.97483	–0.2495	0.00303	–0.2439	0.00546
	HAVCR2	–0.024	0.42419	–0.0263	0.4076	–0.3194	0.00013	–0.3172	0.00027
	GZMB	–0.017	0.56991	–0.0136	0.66762	–0.2446	0.00359	–0.2426	0.0056

BLBC, basal-like breast cancer; COR, correlation coefficient; TAM, tumor-associated macrophage; Th, T-helper; Tfh, follicular helper T; Treg, regulatory cells; CD, cluster of differentiation; FCRL2, Fc receptor like 2; MS4A1, membrane spanning 4-domains A1; FCGR3B, Fc gamma receptor IIIb; CEACAM, CEA cell adhesion molecule; SIGLEC5, sialic acid binding Ig like lectin 5; FPR1, formyl peptide receptor 1; CSF3R, colony stimulating factor 3 receptor; S100A12, S100 calcium binding protein A12; ITGAM, ntegrin subunit alpha M; CCR, C-C motif chemokine receptor; KIR2DL, killer cell immunoglobulin like receptor, two Ig domains and long cytoplasmic tail; KIR3DL, killer cell immunoglobulin-like receptor with three domains and long cytoplasmic tail; KIR2DS4, killer cell immunoglobulin like receptor, two Ig domains and short cytoplasmic tail 4; NCR1, natural cytotoxicity triggering receptor 1; C3AR1, complement C3a receptor 1; CSF1R, colony stimulating factor 1 receptor; CCL2, C-C motif chemokine ligand 2; IL, interleukin; NOS2, nitric oxide synthase 2; IRF5, interferon regulatory factor 5; PTGS2, prostaglandin-endoperoxide synthase 2; VSIG4, V-set and immunoglobulin domain containing 4; MS4A4A, membrane spanning 4-domains A4A; HLA-DPB1, major histocompatibility complex, class II, DP beta 1; HLA-DQB1, major histocompatibility complex, class II, DQ beta 1; HLA-DRA, major histocompatibility complex, class II, DR alpha; HLA-DPA1, major histocompatibility complex, class II, DP alpha 1; NRP1, neuropilin 1; ITGAX, integrin subunit alpha X; TBX21, T-box transcription factor 21; STAT, signal transducer and activator of transcription; IFNG, interferon gamma; TNF, tumor necrosis factor; GATA3, GATA binding protein 3; BCL6, B cell leukemia transcription repressor; FOXP3, forkhead box P3; TGFB1, transforming growth factor beta 1; PDCD1, programmed cell death 1; CTLA4, cytotoxic T-lymphocyte associated protein 4; LAG3, lymphocyte activating 3; HAVCR2, hepatitis A virus cellular receptor 2; GZMB, granzyme B.

of *HOXC10* were significantly higher in brain and CNS, breast, cervical, colorectal, esophageal, gastric, lung, and sarcoma cancer tissues than normal tissues (see *Figure 1A*). Conversely, the expression of *HOXC10* was observed to be lower in kidney, melanoma, and ovarian cancer tissues than normal tissues in some data sets. The results of the TIMER database analysis indicated that *HOXC10* expression was significantly higher in BRCA, ESCA, GBM, HNSC, LUAD, LUSC, STAD, and THCA tissues than adjacent normal tissues, while *HOXC10* expression was significantly lower in KICH and PRAD tissues than adjacent normal tissues (see *Figure 1B*). To explore the systematic prognostic landscape of *HOXC10* in patients with different types of cancer, we used the PrognoScan, GEPIA, and Kaplan-Meier plotter databases to compare the different survival times of patients with high or low expression levels of *HOXC10*. Our results suggested that *HOXC10* may play opposite roles depending on the cancer cell type. Similarly, the overexpression of *HOXC10*, as a proto-oncogene, has been found to be correlated with the poor prognosis of patients with esophageal squamous cell carcinoma (ESCC) (38), and gastric cancer (39). We found that the higher expression of *HOCX10* was related to better RFS in ovarian cancer patients (P=0.038; see Figure S2B).

In breast cancer research, it has been shown that *HOXC10* is highly expressed in breast cancer patients (18,40). Similarly, all the analyses of the online Oncomine, TIMER, PrognoScan, GEPIA and Kaplan-Meier plotter databases indicated that *HOXC10* acts as an oncogene in breast cancer, and the higher expression of this marker is related to a poor prognosis (see *Figures 1*,*2*). In drug-resistance research, *HOXC10* has been reported to contribute to the chemotherapy resistance of breast cancer via DNA repair by binding to cyclin-dependent kinase 7 and activating the nuclear factor kappa B (NF-κB) pathway (40). Moreover, *HOXC10*, the promoter of which contains the ER response element, was also involved in the aromatase inhibitor-resistance of ER positive breast cancer via the regulation of ERα and ERβ (41). The activity of *HOXC10* is upregulated through estrogen by recruiting the mixed-lineage leukemia (*MLL*) 3 and *MLL4* to the estrogen response factor in the promoter region of *HOXC10* (18). In addition, it has been confirmed that the high expression of the *HOXC10* protein is related to the poor prognosis of ER-

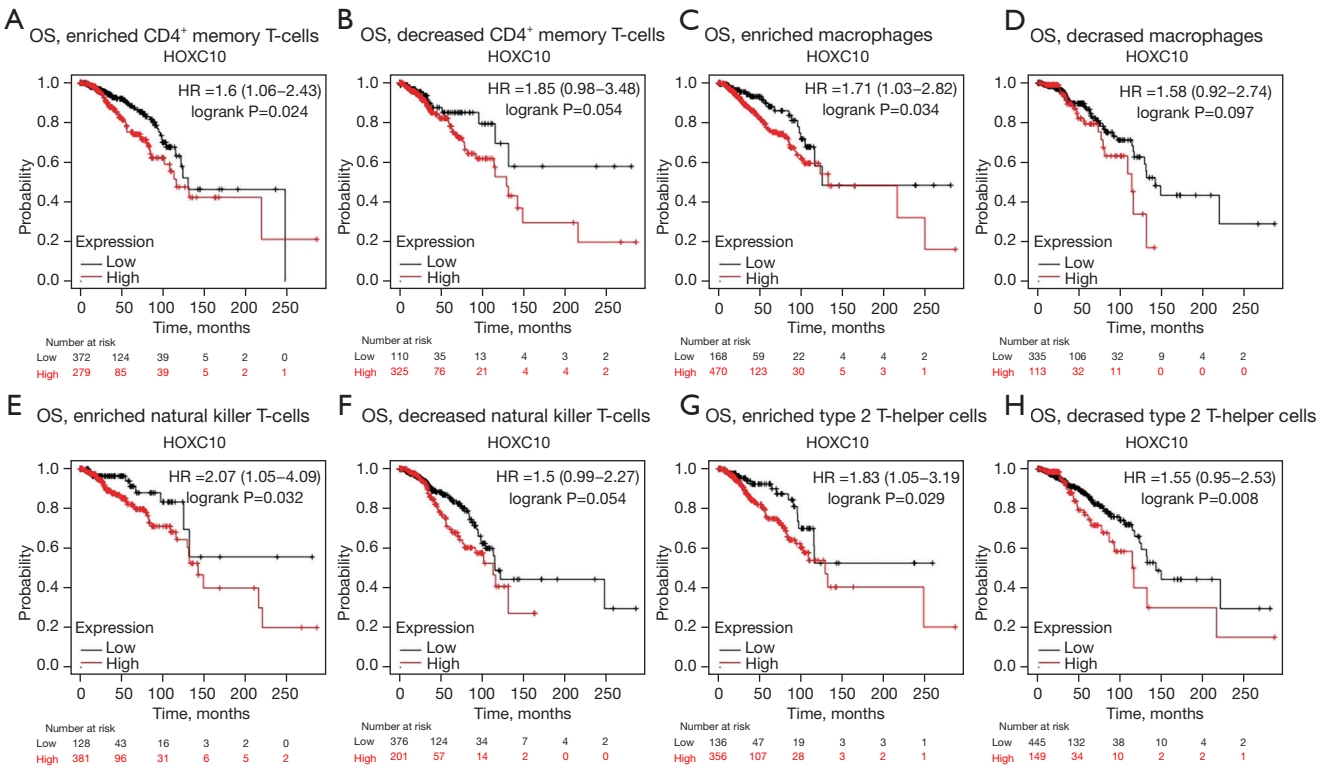

Figure 6 The correlations between *HOXC10* expression and the OS of patients with breast cancer across different subgroups of immune cells based on an analysis of the Kaplan-Meier plotter database. (A,B) The OS curves in enriched CD4+ memory T-cell subgroup and decreased CD4+ memory T-cell subgroup; (C,D) the OS curves in the enriched macrophage subgroup and the decreased macrophage subgroup; (E,F) the OS curves in the enriched NK T-cell subgroup and the decreased NK T-cell subgroup; (G,H) the OS curves in the enriched Th2 cell subgroup and the decreased Th2 cell subgroup. OS, overall survival; CD, cluster of differentiation; NK, natural killer; Th, T-helper.

negative breast cancer patients (40). However, the specific role of *HOXC10* in BLBC remains poorly understood. The Kaplan-Meier plotter database was analyzed by filtering the intrinsic subtype of breast cancer to evaluate the relationship between *HOXC10* expression and the outcomes of patients with BLBC. The median OS of BLBC patients with high *HOXC10* expression was significantly shorter than that of those with low expression (HR =1.97%, 95% CI: 1–3.87; P=0.045; see *Figure 3A*). The prognostic effect of *HOXC10* was also shown in relation to the PPS of BLBC patients (HR =2.14%, 95% CI: 1.02–4.47, P=0.04; see *Figure 3B*), which indicates that *HOXC10* could serve as a biomarker for predicting the prognosis of BLBC patients.

In our results, the analysis of the Kaplan-Meier plotter database based on different intrinsic subtypes of breast cancer showed that the elevated expression of *HOXC10* had adverse effects on both OS and PPS in lymph-node positive breast cancer patients (P=0.0206 and P=0.0072, respectively), which indicates that tumor infiltration might be related to the prognosis of breast cancer. Some researchers have compared the expression levels of *HOXC10* between lymph-node positive and lymph-node negative breast cancer and found that *HOXC10* expression was upregulated in patients with positive lymph nodes (42). The related prognosis and possible immune mechanisms of *HOXC10* in BRCA, especially in BLBC, are still ambiguous. Thus, we investigated whether *HOXC10* was positively correlated to the immune infiltration of macrophages in BLBC (see *Figure 4B*). The *C3AR1*, *CD86* and *CSF1R* of monocytes, the *CD68* and *IL10* of TAMs, the *CD163*, *VSIG4* and *MS4A4A* of M2 macrophages, and the *IRF5* of M1 macrophages were significantly correlated with the expression levels of *HOXC10* in BLBC (see *Table 2*). Thus, *HOXC10* appears to be closely related to macrophage

polarization in BLBC, which further confirms that expressions in BLBC are correlated to immune infiltration. Recent studies have examined the possible mechanisms by which *HOXC10* is related to the immune infiltration and the poor prognosis of patients with different types of cancer. In glioma cells, *HOXC10* was found to induce the expression of immunosuppressive genes, including transforming growth factor-β (TGF-β) programmed death ligand 2, CCL2, and tryptophan 2,3-dioxygenase (20). When the expression of *HOXC10* in gastric cancer cells was overexpressed by transfected overexpression plasmids *in vitro* and *in vivo*, the expression of interleukin-6, tumor necrosis factor-α (TNF-α), TGF-β, and the epidermal growth factor related to the tumor microenvironment were increased (43). In hepatocellular carcinoma, interleukin-1β was found to induce the expression of *HOXC10*, which in turn promoted metastasis by upregulating 3-phosphoinositide dependent protein kinase-1 and vasodilator-stimulated phosphoprotein expression (44). Li *et al.* found that *HOXC10* interacted with its antisense transcript partner lncHOXC-AS3 to regulate the osteogenesis of MES stromal cells derived from the bone marrow of patients with multiple myeloma (45). In oral squamous cell carcinoma, *HOXC10* was found to induce migration and invasion by regulating the drosophila wingless gene and mouse DNA integration site-1 gene family (Wnt)/epithelial-MES transition signaling pathway (46). Thus, interactions between *HOXC10* and the tumor microenvironment could be related to correlations between *HOXC10* expression and immune infiltration and the poor prognosis of BLBC patients.

In summary, increased *HOXC10* expression was found to be correlated with poor prognosis and increased immune-infiltration levels of macrophages in BLBC. HOXC10 expression may contribute to the regulation of monocytes, TAMs, M1 macrophages, and M2 macrophages. Thus, *HOXC10* appears to play an important role in immune-cell infiltration and could serve as a prognosis biomarker in patients with BLBC.

Acknowledgements

Funding: This study was supported by the National Natural Science Foundation of China (Grant No. 81702623) and the Science & Technology Development Fund of Tianjin Education Commission for Higher Education, Tianjin, China.

Footnote

Reporting Checklist: The authors have completed the REMARK reporting checklist. Available at https://atm.amegroups.com/article/view/10.21037/atm-21-6611/rc

Conflicts of Interest: All authors have completed the ICMJE uniform disclosure form (available at https://atm.amegroups.com/article/view/10.21037/atm-21-6611/coif). The authors have no conflicts of interest to declare.

Ethical Statement: The authors are accountable for all aspects of the work in ensuring that questions related to the accuracy or integrity of any part of the work are appropriately investigated and resolved. The study was conducted in accordance with the Declaration of Helsinki (as revised in 2013).

References

1. Siegel RL, Miller KD, Jemal A. Cancer statistics, 2020. CA Cancer J Clin 2020;70:7-30.
2. Lu JT, Tan CC, Wu XR, et al. FOXF2 deficiency accelerates the visceral metastasis of basal-like breast cancer by unrestrictedly increasing TGF-β and miR-182-5p. Cell Death Differ 2020;27:2973-87.
3. Li H, Zhu Y, Burnside ES, et al. Quantitative MRI radiomics in the prediction of molecular classifications of breast cancer subtypes in the TCGA/TCIA data set. NPJ Breast Cancer 2016.
4. Sørlie T, Perou CM, Tibshirani R, et al. Gene expression patterns of breast carcinomas distinguish tumor subclasses with clinical implications. Proc Natl Acad Sci U S A 2001;98:10869-74.
5. Perou CM, Sørlie T, Eisen MB, et al. Molecular portraits of human breast tumours. Nature 2000;406:747-52.
6. Kreike B, van Kouwenhove M, Horlings H, et al. Gene expression profiling and histopathological characterization of triple-negative/basal-like breast carcinomas. Breast Cancer Res 2007;9:R65.
7. Rakha EA, Reis-Filho JS, Ellis IO. Basal-like breast cancer:

a critical review. J Clin Oncol 2008;26:2568-81.
8. Bartmann C, Wischnewsky M, Stüber T, et al. Pattern of metastatic spread and subcategories of breast cancer. Arch Gynecol Obstet 2017;295:211-23.
9. Faiella A, Zappavigna V, Mavilio F, et al. Inhibition of retinoic acid-induced activation of 3' human HOXB genes by antisense oligonucleotides affects sequential activation of genes located upstream in the four HOX clusters. Proc Natl Acad Sci U S A 1994;91:5335-9.
10. Zeltser L, Desplan C, Heintz N. Hoxb-13: a new Hox gene in a distant region of the HOXB cluster maintains colinearity. Development 1996;122:2475-84.
11. Cantile M, Cindolo L, Napodano G, et al. Hyperexpression of locus C genes in the HOX network is strongly associated in vivo with human bladder transitional cell carcinomas. Oncogene 2003;22:6462-8.
12. Shah N, Sukumar S. The Hox genes and their roles in oncogenesis. Nat Rev Cancer 2010;10:361-71.
13. Abate-Shen C. Deregulated homeobox gene expression in cancer: cause or consequence? Nat Rev Cancer 2002;2:777-85.
14. Tan Z, Chen K, Wu W, et al. Overexpression of HOXC10 promotes angiogenesis in human glioma via interaction with PRMT5 and upregulation of VEGFA expression. Theranostics 2018;8:5143-58.
15. Apiou F, Flagiello D, Cillo C, et al. Fine mapping of human HOX gene clusters. Cytogenet Cell Genet 1996;73:114-5.
16. Falaschi A, Abdurashidova G, Biamonti G. DNA replication, development and cancer: a homeotic connection? Crit Rev Biochem Mol Biol 2010;45:14-22.
17. Marchetti L, Comelli L, D'Innocenzo B, et al. Homeotic proteins participate in the function of human-DNA replication origins. Nucleic Acids Res 2010;38:8105-19.
18. Ansari KI, Hussain I, Kasiri S, et al. HOXC10 is overexpressed in breast cancer and transcriptionally regulated by estrogen via involvement of histone methylases MLL3 and MLL4. J Mol Endocrinol 2012;48:61-75.
19. Tang XL, Ding BX, Hua Y, et al. HOXC10 Promotes the Metastasis of Human Lung Adenocarcinoma and Indicates Poor Survival Outcome. Front Physiol 2017;8:557.
20. Li S, Zhang W, Wu C, et al. HOXC10 promotes proliferation and invasion and induces immunosuppressive gene expression in glioma. FEBS J 2018;285:2278-91.
21. Xie X, Xiao Y, Huang X. Homeobox C10 knockdown suppresses cell proliferation and promotes cell apoptosis in osteosarcoma cells through regulating caspase 3. Onco Targets Ther 2018;11:473-82.
22. Zhai Y, Kuick R, Nan B, et al. Gene expression analysis of preinvasive and invasive cervical squamous cell carcinomas identifies HOXC10 as a key mediator of invasion. Cancer Res 2007;67:10163-72.
23. Feng X, Li T, Liu Z, et al. HOXC10 up-regulation contributes to human thyroid cancer and indicates poor survival outcome. Mol Biosyst 2015;11:2946-54.
24. Rhodes DR, Kalyana-Sundaram S, Mahavisno V, et al. Oncomine 3.0: genes, pathways, and networks in a collection of 18,000 cancer gene expression profiles. Neoplasia 2007;9:166-80.
25. Mizuno H, Kitada K, Nakai K, et al. PrognoScan: a new database for meta-analysis of the prognostic value of genes. BMC Med Genomics 2009;2:18.
26. Tang Z, Li C, Kang B, et al. GEPIA: a web server for cancer and normal gene expression profiling and interactive analyses. Nucleic Acids Res 2017;45:W98-W102.
27. Győrffy B, Lanczky A, Eklund AC, et al. An online survival analysis tool to rapidly assess the effect of 22,277 genes on breast cancer prognosis using microarray data of 1,809 patients. Breast Cancer Res Treat 2010;123:725-31.
28. Li T, Fan J, Wang B, et al. TIMER: A Web Server for Comprehensive Analysis of Tumor-Infiltrating Immune Cells. Cancer Res 2017;77:e108-10.
29. Tomczak K, Czerwińska P, Wiznerowicz M. The Cancer Genome Atlas (TCGA): an immeasurable source of knowledge. Contemp Oncol (Pozn) 2015;19:A68-77.
30. Pan JH, Zhou H, Cooper L, et al. LAYN Is a Prognostic Biomarker and Correlated With Immune Infiltrates in Gastric and Colon Cancers. Front Immunol 2019;10:6.
31. Tu L, Guan R, Yang H, et al. Assessment of the expression of the immune checkpoint molecules PD-1, CTLA4, TIM-3 and LAG-3 across different cancers in relation to treatment response, tumor-infiltrating immune cells and survival. Int J Cancer 2020;147:423-39.
32. Denkert C, von Minckwitz G, Darb-Esfahani S, et al. Tumour-infiltrating lymphocytes and prognosis in different subtypes of breast cancer: a pooled analysis of 3771 patients treated with neoadjuvant therapy. Lancet Oncol 2018;19:40-50.
33. Tekpli X, Lien T, Røssevold AH, et al. An independent poor-prognosis subtype of breast cancer defined by a distinct tumor immune microenvironment. Nat Commun 2019;10:5499.
34. Stanton SE, Disis ML. Clinical significance of tumor-infiltrating lymphocytes in breast cancer. J Immunother Cancer 2016;4:59.

35. Carlson MR, Komine Y, Bryant SV, et al. Expression of Hoxb13 and Hoxc10 in developing and regenerating Axolotl limbs and tails. Dev Biol 2001;229:396-406.
36. Hostikka SL, Gong J, Carpenter EM. Axial and appendicular skeletal transformations, ligament alterations, and motor neuron loss in Hoxc10 mutants. Int J Biol Sci 2009;5:397-410.
37. Yao S, He L, Zhang Y, et al. HOXC10 promotes gastric cancer cell invasion and migration via regulation of the NF-κB pathway. Biochem Biophys Res Commun 2018;501:628-35.
38. Suo D, Wang Z, Li L, et al. HOXC10 upregulation confers resistance to chemoradiotherapy in ESCC tumor cells and predicts poor prognosis. Oncogene 2020;39:5441-54.
39. Miwa T, Kanda M, Umeda S, et al. Homeobox C10 Influences on the Malignant Phenotype of Gastric Cancer Cell Lines and its Elevated Expression Positively Correlates with Recurrence and Poor Survival. Ann Surg Oncol 2019;26:1535-43.
40. Sadik H, Korangath P, Nguyen NK, et al. HOXC10 Expression Supports the Development of Chemotherapy Resistance by Fine Tuning DNA Repair in Breast Cancer Cells. Cancer Res 2016;76:4443-56.
41. Pathiraja TN, Nayak SR, Xi Y, et al. Epigenetic reprogramming of HOXC10 in endocrine-resistant breast cancer. Sci Transl Med 2014;6:229ra41.
42. Abba MC, Sun H, Hawkins KA, et al. Breast cancer molecular signatures as determined by SAGE: correlation with lymph node status. Mol Cancer Res 2007;5:881-90.
43. Li J, Tong G, Huang C, et al. HOXC10 promotes cell migration, invasion, and tumor growth in gastric carcinoma cells through upregulating proinflammatory cytokines. J Cell Physiol 2020;235:3579-91.
44. Dang Y, Chen J, Feng W, et al. Interleukin 1β-mediated HOXC10 Overexpression Promotes Hepatocellular Carcinoma Metastasis by Upregulating PDPK1 and VASP. Theranostics 2020;10:3833-48.
45. Li B, Han H, Song S, et al. HOXC10 Regulates Osteogenesis of Mesenchymal Stromal Cells Through Interaction with Its Natural Antisense Transcript lncHOXC-AS3. Stem Cells 2019;37:247-56.
46. Dai BW, Yang ZM, Deng P, et al. HOXC10 promotes migration and invasion via the WNT-EMT signaling pathway in oral squamous cell carcinoma. J Cancer 2019;10:4540-51.

Cite this article as: Zhang X, Zheng Y, Liu X, Wang K, Zhao H, Yin Y, Yu Y. The expression of *HOXC10* is correlated with tumor-infiltrating immune cells in basal-like breast cancer and serves as a prognostic biomarker. Ann Transl Med 2022;10(2):81. doi: 10.21037/atm-21-6611

Supplementary

Table S1 The mRNA expression of HOXC10 between cancer and normal tissues in the Oncomine database

Cancer	Cancer type	P value	Fold change	Rank (%)	Sample	Reference (PMID)
Bladder	Infiltrating bladder urothelial carcinoma	9.28E-04	–1.579	21%	27	15173019
Brain and CNS	Brain glioblastoma	2.19E-10	2.087	4%	552	TCGA
	Glioblastoma	9.90E-10	2.413	8%	104	16616334
	Glioblastoma	2.37E-07	1.505	4%	84	18565887
	Glioblastoma	6.14E-05	2.171	8%	23	16204036
Breast	Invasive ductal breast carcinoma	2.92E-30	3.28	4%	450	TCGA
	Invasive breast carcinoma	6.67E-20	3.655	3%	137	TCGA
	Invasive lobular breast carcinoma	1.87E-14	4.239	2%	97	TCGA
	Invasive ductal and lobular breast carcinoma	3.87E-05	8.303	4%	64	TCGA
	Invasive breast carcinoma stroma	2.04E-11	1.992	11%	59	18438415
	Invasive breast carcinoma	3.41E-05	1.595	3%	158	21373875
Cervical	Cervical squamous cell carcinoma epithelia	4.12E-06	2.949	3%	31	17974957
Colorectal	Rectosigmoid adenocarcinoma	1.77E-12	2.305	1%	25	TCGA
	Colon adenocarcinoma	2.16E-08	1.542	17%	123	TCGA
	Cecum adenocarcinoma	2.43E-07	1.696	11%	44	TCGA
	Colon mucinous adenocarcinoma	5.10E-05	1.538	18%	44	TCGA
	Rectal mucinous adenocarcinoma	3.77E-4	1.802	9%	28	TCGA
Esophageal	Esophageal squamous cell carcinoma	1.91E-13	1.658	4%	106	21385931
	Esophageal squamous cell carcinoma	2.51E-07	3.357	3%	34	20955586
Gastric	Gastric intestinal type adenocarcinoma	1.9E-06	3.768	13%	57	19081245
Kidney	Renal pelvis urothelial carcinoma	1.3E-05	–2.86	10%	31	16115910
Lung	Lung adenocarcinoma	1.08E-07	1.668	13%	246	22080568
	Lung adenocarcinoma	2.55E-6	1.982	13%	110	20421987
	Squamous cell lung carcinoma	6.16E-05	1.812	19%	92	20421987
	Large cell lung carcinoma	4.40E-04	3.265	17%	84	20421987
Melanoma	Benign melanocytic skin nevus	9.72E-7	–3.406	1%	25	16243793
	Cutaneous melanoma	3.62E-04	–1.74	13%	52	16243793
Ovarian	Ovarian serous adenocarcinoma	2.28E-07	–10.535	9%	48	19486012
Pancreatic	Pancreatic carcinoma	1.77E-04	1.769	10%	52	19732725
Sarcoma	Myxoid/round cell liposarcoma	1.24E-04	2.773	20%	29	20601955
	Leiomyosarcoma	7.73E-04	2.409	22%	35	20601955
	Round cell liposarcoma	1.83E-04	6.037	4%	19	15994966
Other	Vulvar intraepithelial neoplasia	2.76E-04	–1.839	3%	19	17471573

CNS, central nervous system; TCGA, The Cancer Genome Atlas; PMID, PubMed Identifier.

https://dx.doi.org/10.21037/atm-21-6611

Table S2 The relationships between the expression of HOXC10 and the prognoses of different cancers in the PrognoScan database

Cancer type	Subtype	Data set	End point	N	Cox P value	HR [95% CI-low CI-upp]
Bladder cancer	–	GSE5287	OS	30	0.109862	1.36 [0.93–2.00]
	–	GSE13507	OS	165	0.417422	1.37 [0.64–2.92]
	Transitional cell carcinoma	GSE13507	DSS	165	0.389573	1.58 [0.56–4.44]
Blood cancer	AML	GSE12417-GPL96	OS	163	0.560195	0.73 [0.25–2.12]
	AML	GSE12417-GPL570	OS	79	0.646702	0.69 [0.14–3.32]
	AML	GSE5122	OS	58	0.92701	0.98 [0.71–1.37]
	AML	GSE8970	OS	34	0.131566	0.63 [0.35–1.15]
	B-cell lymphoma	GSE4475	OS	158	0.151152	3.23 [0.65–16.02]
	DLBCL	E-TABM-346	OS	53	0.09165	0.69 [0.44–1.06]
	DLBCL	E-TABM-346	EFS	53	0.100929	0.72 [0.48–1.07]
	Follicular lymphoma	GSE16131-GPL96	OS	180	0.63917	0.94 [0.74–1.20]
	Multiple myeloma	GSE2658	DSS	559	0.321423	1.17 [0.85–1.61]
Brain cancer	Astrocytoma	GSE4271-GPL96	OS	77	0.028386	1.34 [1.03–1.75]
	Glioblastoma	GSE7696	OS	70	0.57152	1.14 [0.72–1.81]
	Glioma	GSE4412-GPL96	OS	74	0.059568	1.54 [0.98–2.41]
	Meningioma	GSE16581	OS	67	0.137701	0.03 [0.00–3.21]
Breast cancer	–	GSE19615	DMFS	115	0.481287	1.23 [0.69–2.22]
	–	GSE12276	PFS	204	0.405076	0.95 [0.85–1.07]
	–	GSE6532–GPL570	PFS	87	0.346351	1.10 [0.90–1.34]
	–	GSE6532-GPL570	DMFS	87	0.346351	1.10 [0.90–1.34]
	–	GSE9195	PFS	77	0.428403	1.13 [0.84–1.51]
	–	GSE9195	DMFS	77	0.573515	1.10 [0.79–1.53]
	–	GSE12093	DMFS	136	0.194555	1.32 [0.87–2.00]
	–	GSE11121	DMFS	200	0.435395	1.15 [0.81–1.63]
	–	GSE1378	PFS	60	0.024856	1.27 [1.03–1.56]
	–	GSE1379	PFS	60	0.036064	1.25 [1.01–1.54]
	–	GSE9893	OS	155	0.309388	0.89 [0.70–1.12]
	–	GSE2034	DMFS	286	0.759514	1.03 [0.85–1.24]
	–	GSE1456-GPL96	OS	159	0.480164	0.87 [0.59–1.28]
	–	GSE1456-GPL96	PFS	159	0.186285	1.30 [0.88–1.93]
	–	GSE1456-GPL96	DSS	159	0.222686	1.34 [0.84–2.14]
	–	GSE7378	DFS	54	0.273791	1.25 [0.84–1.85]
	–	E-TABM-158	DMFS	117	0.879649	1.02 [0.80–1.30]
	–	E-TABM-158	OS	117	0.751855	1.03 [0.85–1.26]
	–	E-TABM-158	PFS	117	0.751855	1.03 [0.85–1.26]
	–	E-TABM-158	DSS	117	0.971632	1.00 [0.80–1.26]

Table S2 (*continued*)

https://dx.doi.org/10.21037/atm-21-6611

Table S2 (*continued*)

Cancer type	Subtype	Data set	End point	N	Cox P value	HR [95% CI-low CI-upp]
	–	GSE3494-GPL96	DSS	236	0.35915	1.14 [0.86–1.51]
		GSE4922-GPL96	DFS	249	0.270416	1.13 [0.91–1.42]
	–	GSE2990	DMFS	125	0.482258	1.12 [0.82–1.52]
	-	GSE2990	PFS	125	0.773579	1.04 [0.82–1.31]
	–	GSE2990	DMFS	54	0.334923	0.86 [0.64–1.16]
	–	GSE2990	PFS	62	0.276037	0.87 [0.69–1.11]
	–	GSE7390	PFS	198	0.223364	0.91 [0.78–1.06]
	–	GSE7390	DMFS	198	0.802096	0.98 [0.82–1.16]
	–	GSE7390	OS	198	0.939142	0.99 [0.83–1.19]
Colorectal cancer	–	GSE12945	DFS	51	0.405093	4.41 [0.13–145.01]
	–	GSE12945	OS	62	0.109194	5.46 [0.68–43.58]
	–	GSE17536	OS	177	0.896046	1.06 [0.43–2.60]
	–	GSE17536	DFS	145	0.100833	2.59 [0.83–8.10]
	–	GSE17536	DSS	177	0.928002	1.05 [0.38–2.92]
	–	GSE14333	DFS	226	0.098219	1.31 [0.95–1.80]
	-	GSE17537	DFS	55	0.42966	1.69 [0.46–6.16]
	-	GSE17537	DSS	49	0.9424	0.94 [0.18–4.84]
	-	GSE17537	OS	55	0.39347	1.70 [0.50–5.73]
Eye cancer	Uveal melanoma	GSE22138	DMFS	63	0.145495	1.41 [0.89–2.25]
Head and neck cancer	Squamous cell carcinoma	GSE2837	PFS	28	0.83989	1.04 [0.73–1.47]
Lung cancer	Adenocarcinoma	jacob-00182-CANDF	OS	82	0.871072	1.03 [0.74–1.42]
	Adenocarcinoma	jacob-00182-HLM	OS	79	0.221853	0.85 [0.66–1.10]
	Adenocarcinoma	jacob-00182-MSK	OS	104	0.274592	0.81 [0.55–1.18]
	Adenocarcinoma	GSE13213	OS	117	0.820718	1.03 [0.77–1.38]
	Adenocarcinoma	GSE13213	OS	117	0.421591	1.08 [0.90–1.29]
	Adenocarcinoma	GSE31210	OS	204	0.223551	0.78 [0.53–1.16]
	Adenocarcinoma	GSE31210	PFS	204	0.85112	1.03 [0.78–1.36]
	Adenocarcinoma	jacob-00182-UM	OS	178	0.134631	0.88 [0.74–1.04]
	NSCLC	GSE3141	OS	111	0.494625	0.93 [0.74–1.16]
	NSCLC	GSE14814	OS	90	0.136038	1.35 [0.91–2.00]
	NSCLC	GSE14814	DSS	90	0.099858	1.44 [0.93–2.23]
	NSCLC	GSE8894	PFS	138	0.484781	0.95 [0.83–1.10]
	SCC	GSE4573	OS	129	0.984169	1.00 [0.70–1.44]
	SCC	GSE17710	PFS	56	0.500439	0.88 [0.60–1.28]
	SCC	GSE17710	OS	56	0.935506	0.97 [0.42–2.22]

Table S2 (*continued*)

https://dx.doi.org/10.21037/atm-21-6611

Table S2 (*continued*)

Cancer type	Subtype	Data set	End point	N	Cox P value	HR [95% CI-low CI-upp]
	SCC	GSE17710	OS	56	0.404159	0.85 [0.58–1.25]
	SCC	GSE17710	PFS	56	0.705531	0.94 [0.68–1.30]
	SCC	GSE17710	PFS	56	0.81684	0.91 [0.40–2.06]
	SCC	GSE17710	OS	56	0.569059	0.90 [0.64–1.28]
Ovarian cancer	–	GSE9891	OS	278	0.517708	0.94 [0.79–1.13]
	–	DUKE-OC	OS	133	0.830605	0.99 [0.86–1.13]
	–	GSE26712	OS	185	0.010987	1.43 [1.09–1.89]
	–	GSE26712	DFS	185	0.022872	1.36 [1.04–1.77]
	–	GSE17260	OS	110	0.910522	0.99 [0.76–1.27]
	–	GSE17260	OS	110	0.972928	1.00 [0.82–1.23]
	–	GSE17260	PFS	110	0.942258	0.99 [0.82–1.20]
	–	GSE17260	PFS	110	0.952676	1.00 [0.87–1.16]
	–	GSE14764	OS	80	0.609544	1.10 [0.77–1.57]
Skin cancer	Melanoma	GSE19234	OS	38	0.258189	1.35 [0.80–2.25]
Soft tissue cancer	Liposarcoma	GSE30929	DRFS	140	0.703816	0.95 [0.73–1.24]

HR, hazard ratio; CI, confidence interval; AML, acute myelocytic leukemia; DLBCL, diffuse large B cell lymphoma; NSCLC, non-small cell lung cancer; SCC, squamous cell carcinoma; OS, overall survival; DSS, disease-specific survival; EFS, event-free survival; DMFS, distant metastasis-free survival; PFS, progression-free survival; DFS, disease-free survival.

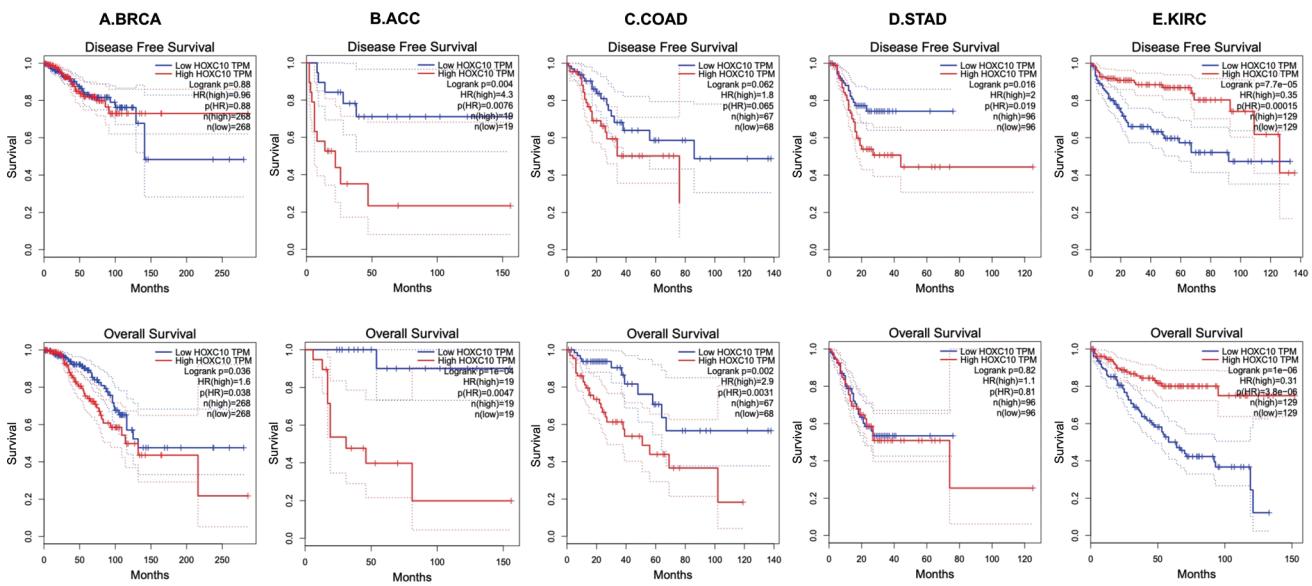

Figure S1 The predictive effect of *HOXC10* in the prognosis of different cancers in the GEPIA database (cutoff: 75–25%). (A) The Kaplan-Meier survival curves of DFS and OS in BRCA; (B) The Kaplan-Meier survival curves of DFS and OS in ACC; (C) The Kaplan-Meier survival curves of DFS and OS in COAD; (D) The Kaplan-Meier survival curves of DFS and OS in STAD; (E) The Kaplan-Meier survival curves of DFS and OS in KIRC. GEPIA, Gene Expression Profiling Interactive Analysis; DFS, disease-free survival; OS, overall survival; BRCA, breast invasive carcinoma; ACC, adrenocortical carcinoma; COAD, colon adenocarcinoma; STAD, stomach adenocarcinoma; KIRC, kidney renal clear cell carcinoma.

https://dx.doi.org/10.21037/atm-21-6611

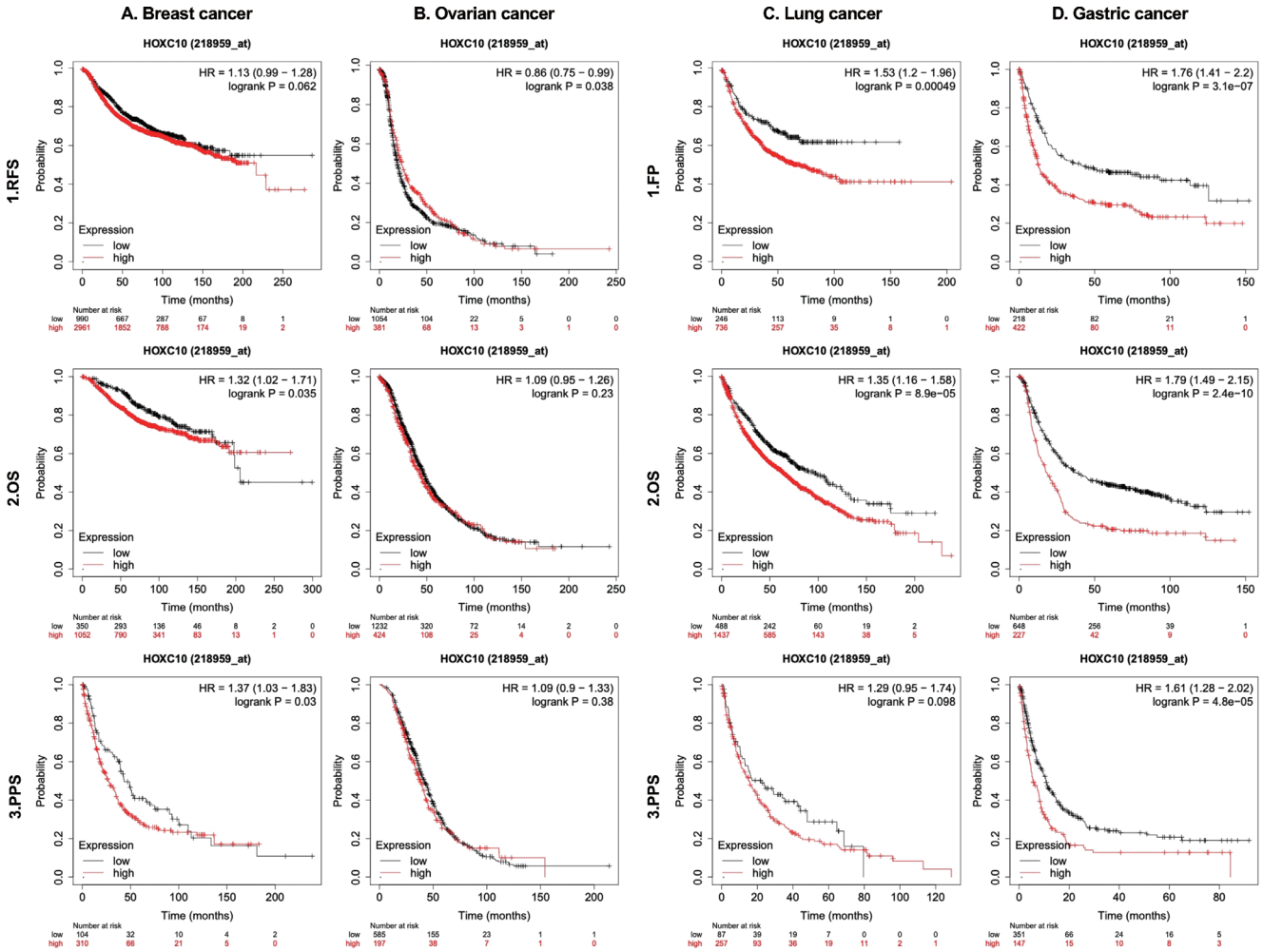

Figure S2 Kaplan-Meier survival curves comparing patients with high expression of *HOXC10* to those with low expression in breast cancer, ovarian cancer, lung cancer, and gastric cancer data sets using the Kaplan-Meier plotter database. (A,B) The Kaplan-Meier survival curves for RFS (A,B-1), OS (A,B-2), and PPS (A,B-3) in breast cancer and ovarian cancer. (C,D) The Kaplan-Meier survival curves for first progression (FP) (C,D-1), OS (C,D-2), and PPS (C,D-3) in lung cancer and gastric cancer. RFS, relapse-free survival; OS, overall survival; PPS, post-progression survival; FP, first progression.

https://dx.doi.org/10.21037/atm-21-6611

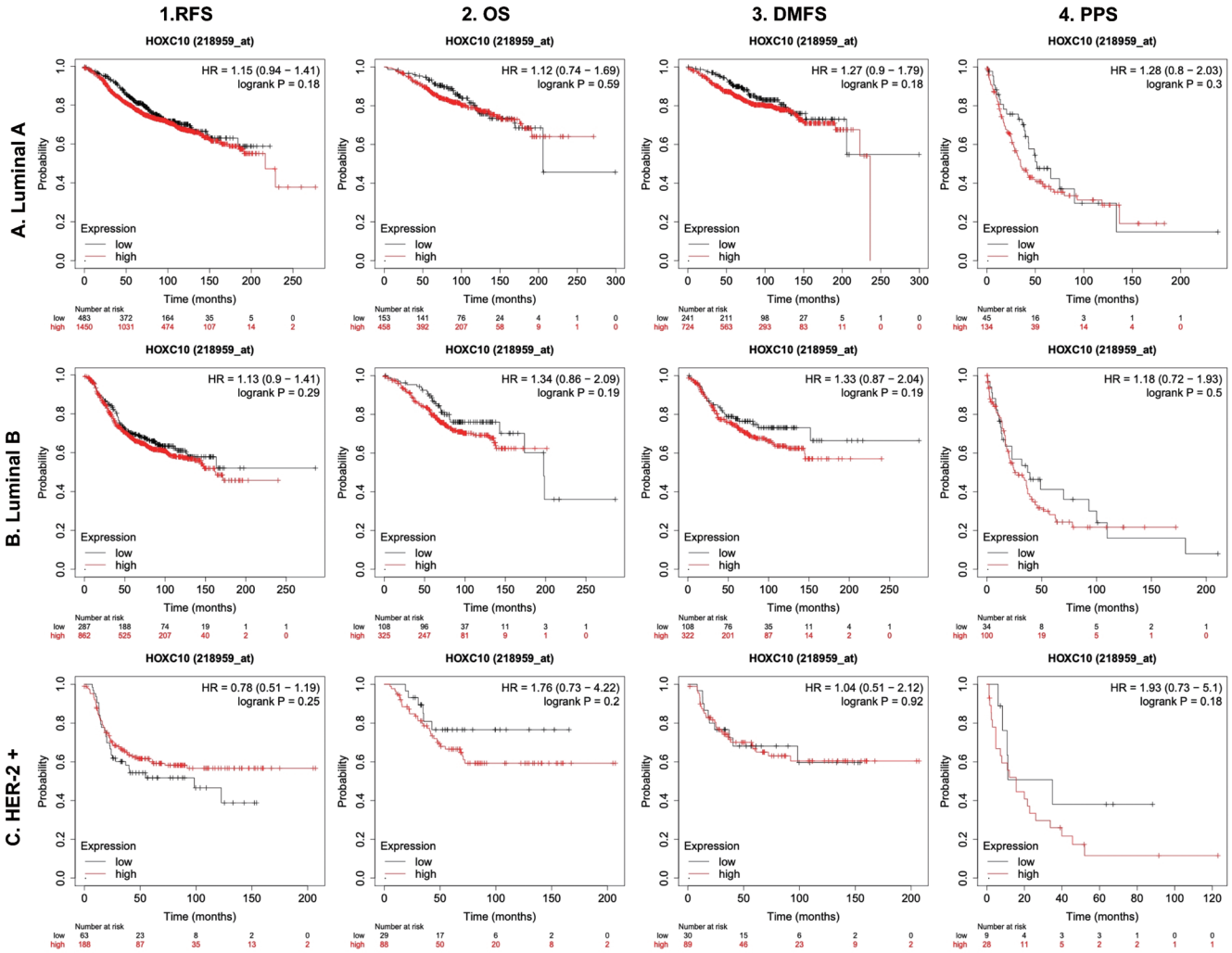

Figure S3 The relationship between the expression of *HOXC10* and the prognosis of different subtypes of breast cancer in the Kaplan-Meier plotter database. (A) The Kaplan-Meier survival curves for RFS, OS, DMFS, and PPS in luminal A breast cancer. (B) The Kaplan-Meier survival curves for RFS, OS, DMFS, and PPS in luminal B breast cancer. (C) The Kaplan-Meier survival curves for RFS, OS, DMFS, and PPS in Her-2+ breast cancer. RFS, relapse-free survival; OS, overall survival; DMFS, distant metastasis-free survival; PPS, post-progression survival; Her-2, human epidermal growth factor receptor 2.

https://dx.doi.org/10.21037/atm-21-6611

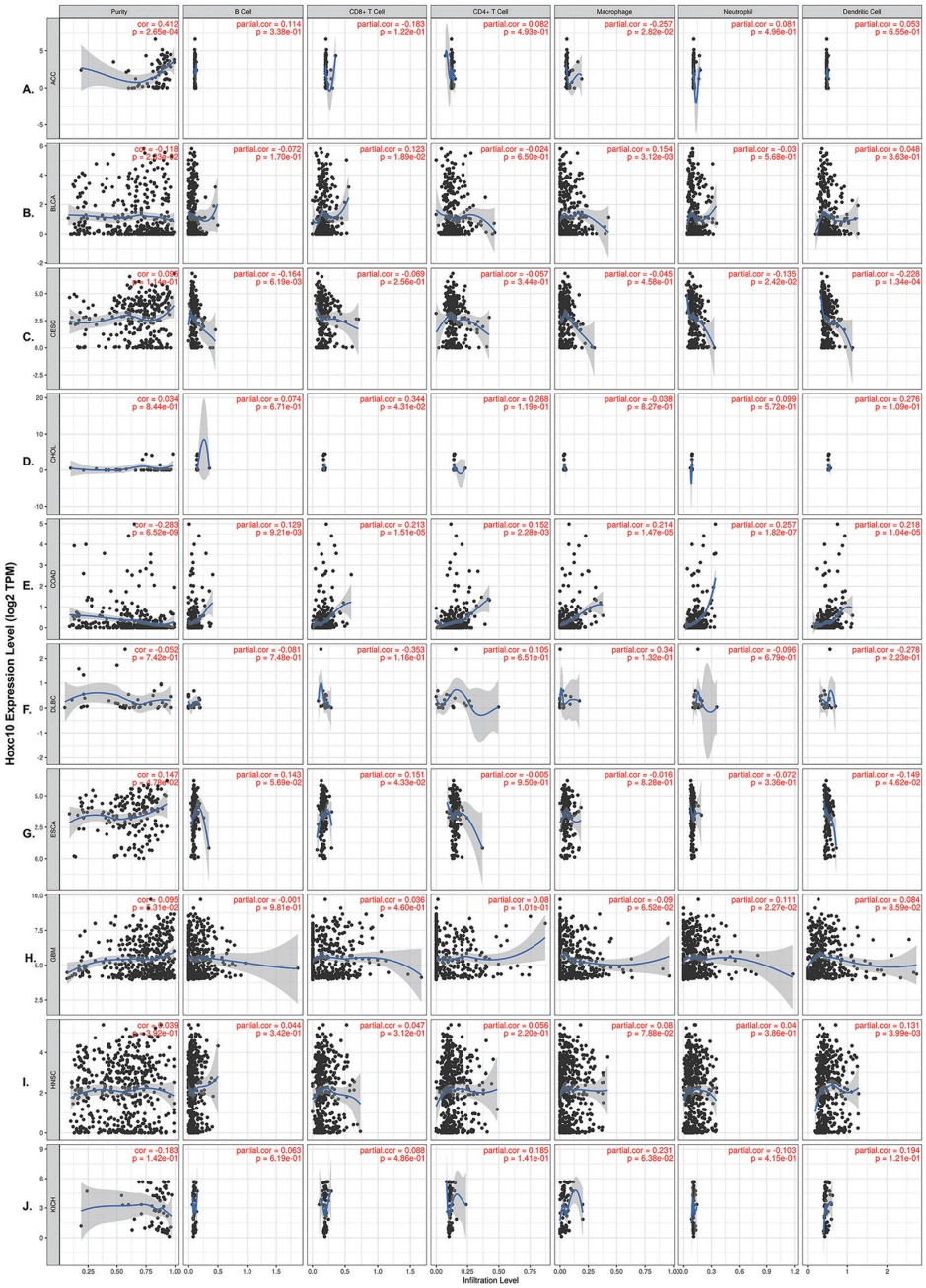

https://dx.doi.org/10.21037/atm-21-6611

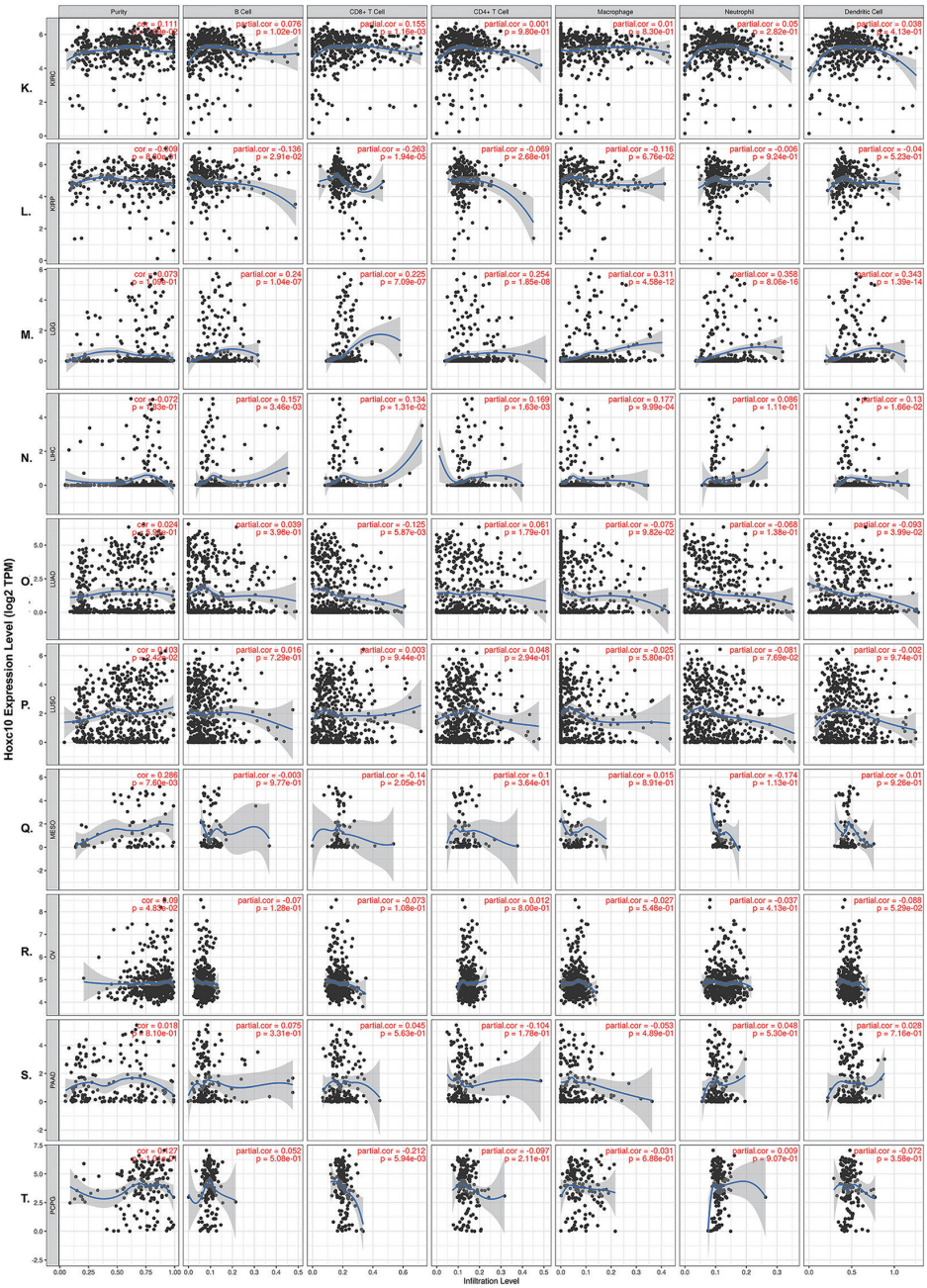

https://dx.doi.org/10.21037/atm-21-6611

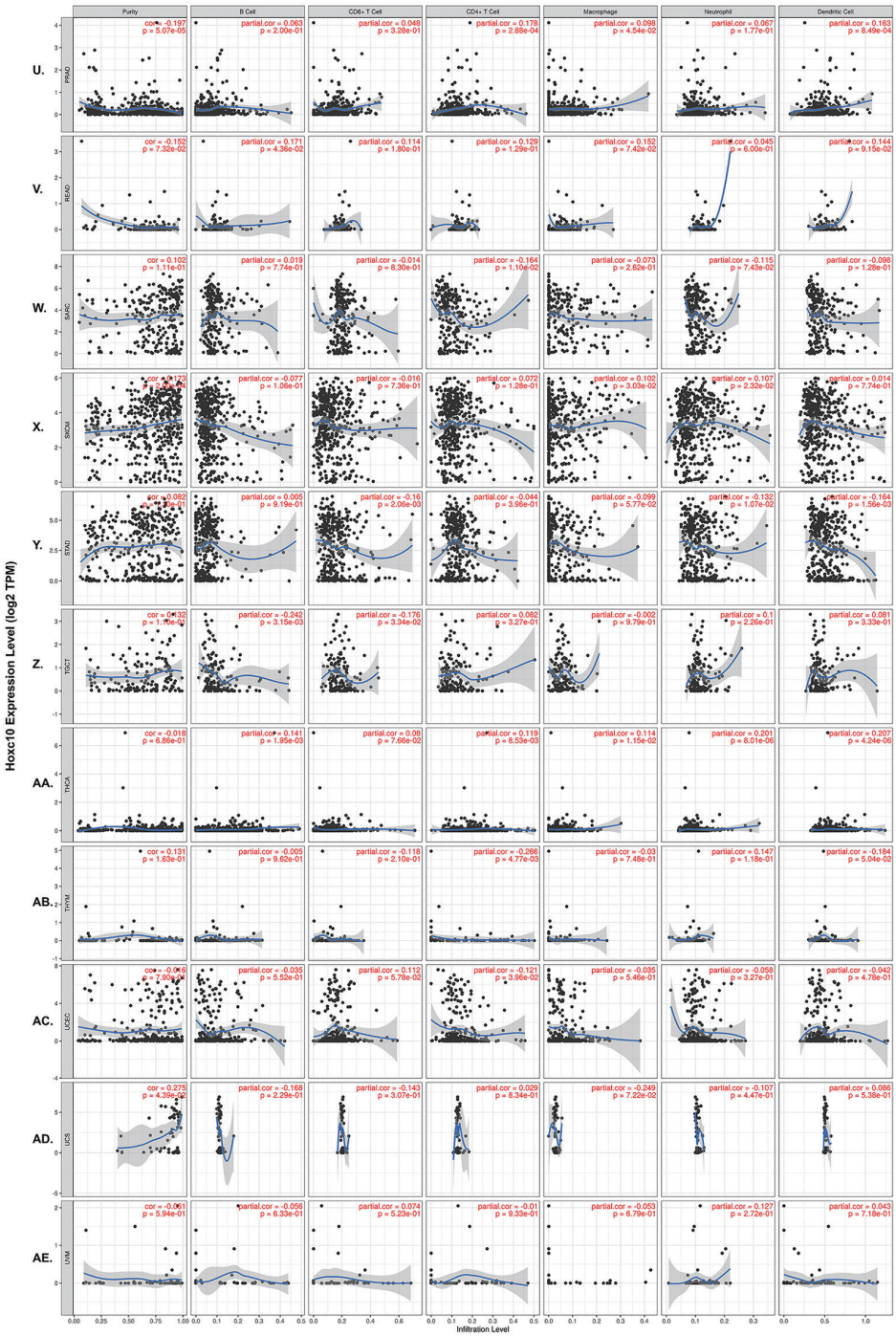

Figure S4 Correlations between *HOXC10* expression and immune infiltration in all other types of cancer, excluding breast cancer, using the Tumor Immune Estimation Resource database. (A) Adrenocortical carcinoma (ACC); (B) bladder urothelial carcinoma (BLCA); (C) cervical squamous cell carcinoma and endocervical adenocarcinoma (CESC); (D) cholangio carcinoma (CHOL); (E) colon adenocarcinoma (COAD); (F) lymphoid neoplasm diffuse large B-cell lymphoma (DLBC); (G) esophageal carcinoma (ESCA); (H) glioblastoma multiforme (GBM); (I) head and neck squamous cell carcinoma (HNSC); (J) kidney chromophobe (KICH); (K) kidney renal clear cell carcinoma (KIRC); (L) kidney renal papillary cell carcinoma (KIRP); (M) brain lower grade glioma (LGG); (N) liver hepatocellular carcinoma (LIHC); (O) lung adenocarcinoma (LUAD); (P) lung squamous cell carcinoma (LUSC); (Q) mesothelioma (MESO); (R) ovarian serous cystadenocarcinoma (OV); (S) pancreatic adenocarcinoma (PAAD); (T) pheochromocytoma and paraganglioma (PCPG); (U) PRAD; (V) rectum adenocarcinoma (READ); (W) sarcoma (SARC); (X) skin cutaneous melanoma (SKCM); (Y) stomach adenocarcinoma (STAD); (Z) testicular germ cell tumors (TGCT); (AA) thyroid carcinoma (THCA); (AB) thymoma (THYM); (AC) uterine corpus endometrial carcinoma (UCEC); (AD) uterine carcinosarcoma (UCS); (AE) uveal melanoma (UVM).

https://dx.doi.org/10.21037/atm-21-6611

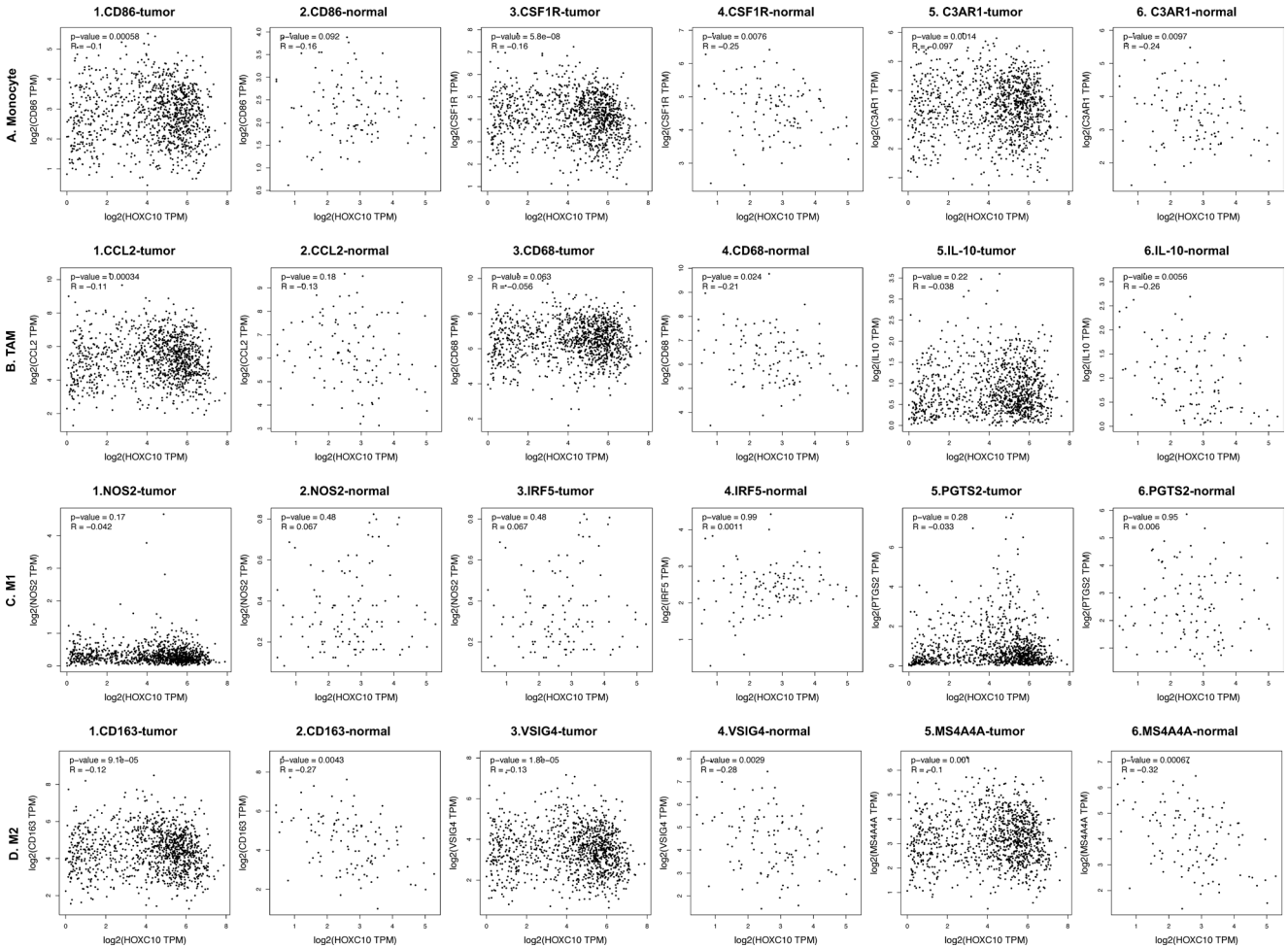

Figure S5 The correlation between *HOXC10* expression and the biomarkers of immune cells in BRCA tumors by GEPIA. (A) Monocytes; (B) TAMs; (C) M1 macrophages; and (D) M2 macrophages. BRCA, breast invasive carcinoma; GEPIA, Gene Expression Profiling Interactive Analysis; TAMs, tumor-associated macrophages.

https://dx.doi.org/10.21037/atm-21-6611

Table S3 The correlations between HOXC10 and genetic markers of infiltrating immune cells in luminal and Her-2+ breast cancer

Description	Gene markers	Luminal Breast Cancer				Her-2 positive Breast Cancer			
		None		Purity		None		Purity	
		COR	P	COR	P	COR	P	COR	P
B-cell	CD19	0.1352	0.00076	0.1535	0.00032	–0.085	0.49229	–0.125	0.34387
	CD79A	0.0835	0.03819	0.1074	0.012	–0.11	0.37612	–0.147	0.26448
	FCRL2	0.0902	0.02523	0.1142	0.00756	–0.033	0.79062	–0.07	0.60057
	MS4A1	0.0805	0.04589	0.1059	0.01326	–0.062	0.61686	–0.097	0.46457
CD8+ T cell	CD8A	0.1003	0.01272	0.1254	0.00332	–0.008	0.94913	–0.05	0.70405
	CD8B	0.1433	0.00037	0.1648	0.00011	–0.057	0.64432	–0.105	0.42858
T cell (general)	CD3D	0.1101	0.00623	0.1386	0.00116	–0.062	0.62004	–0.116	0.3813
	CD3E	0.1166	0.00374	0.1409	0.00096	–0.035	0.77664	–0.086	0.51492
	CD2	0.1245	0.00198	0.1472	0.00057	–0.082	0.50913	–0.125	0.34475
Neutrophils	FCGR3B	0.0136	0.73681	0.0186	0.66398	–0.211	0.08671	–0.214	0.10374
	CEACAM3	0.0762	0.05887	0.1066	0.01266	–0.014	0.91043	–0.091	0.49085
	SIGLEC5	0.0512	0.20457	0.0537	0.21035	–0.376	0.00182	–0.375	0.00361
	FPR1	0.0247	0.54126	0.0342	0.42541	–0.345	0.00447	–0.363	0.00493
	CSF3R	0.0159	0.69394	0.0068	0.87333	–0.024	0.8487	–0.031	0.81613
	S100A12	0.0306	0.44884	0.0473	0.26945	–0.082	0.51201	–0.006	0.96547
	CEACAM8	–0.008	0.83701	0.0204	0.6336	0.013	0.91553	0.0102	0.93897
	ITGAM	0.0586	0.14603	0.0497	0.24602	–0.372	0.00204	–0.383	0.00292
	CCR7	0.0922	0.02216	0.1107	0.00967	0.044	0.72202	–0.015	0.90859
Natural killer cells	KIR2DL1	0.0064	0.87377	0.0535	0.21171	–8E-04	0.99488	0.0591	0.65659
	KIR2DL3	0.0004	0.9925	0.0314	0.46361	0.002	0.98407	–0.007	0.96032
	KIR2DL4	0.0404	0.31722	0.0701	0.10166	–0.012	0.92174	–0.066	0.6196
	KIR3DL1	0.0174	0.66563	0.0373	0.38423	–0.015	0.90245	–0.045	0.73453
	KIR3DL2	0.0344	0.3947	0.0597	0.16393	0.022	0.86202	–0.001	0.99192
	KIR3DL3	–0.055	0.17198	–0.032	0.453	0.127	0.30583	0.1529	0.24768
	KIR2DS4	–0.01	0.79973	0.0274	0.52245	–0.05	0.68727	–0.006	0.96653
	NCR1	–0.004	0.9292	–3E-04	0.99453	–0.116	0.34891	–0.129	0.3295
Monocytes	C3AR1	0.0047	0.90771	0.0099	0.81748	–0.315	0.0098	–0.335	0.00972
	CD86	0.0485	0.22904	0.0628	0.14272	–0.245	0.04594	–0.27	0.03889
	CSF1R	–0.069	0.08879	–0.057	0.18521	–0.299	0.01411	–0.317	0.01492
TAM	CCL2	0.0614	0.12767	0.0854	0.046	–0.123	0.32123	–0.188	0.1538
	CD68	0.0792	0.04943	0.0818	0.05625	–0.351	0.0038	–0.354	0.00618
	IL10	0.1036	0.01009	0.1162	0.00658	–0.178	0.14987	–0.198	0.13278

Table S3 (*continued*)

https://dx.doi.org/10.21037/atm-21-6611

Table S3 (*continued*)

Description	Gene markers	Luminal Breast Cancer				Her-2 positive Breast Cancer			
		None		Purity		None		Purity	
		COR	P	COR	P	COR	P	COR	P
M1 macrophage	NOS2	–0.09	0.02612	–0.097	0.02338	–0.269	0.02789	–0.281	0.03143
	IRF5	–0.02	0.61896	–0.019	0.6656	–0.179	0.14611	–0.16	0.22555
	PTGS2	0.0436	0.28007	0.0469	0.27382	–0.12	0.33129	–0.111	0.39992
M2 macrophage	CD163	0.0014	0.97143	0.0188	0.66044	–0.332	0.00634	–0.336	0.0095
	VSIG4	–0.055	0.17269	–0.046	0.28762	–0.323	0.00796	–0.272	0.0376
	MS4A4A	0.0409	0.31125	0.0583	0.17351	–0.305	0.01235	–0.316	0.01518
	KIR2DS4	–0.01	0.79973	0.0274	0.52245	–0.05	0.68727	–0.006	0.96653
Dendritic cells	HLA-DPB1	0.0109	0.78641	0.0238	0.57945	–0.135	0.27646	–0.203	0.12328
	HLA-DQB1	0.0295	0.46443	0.0254	0.55354	–0.15	0.22358	–0.253	0.05332
	HLA-DRA	0.0719	0.07474	0.082	0.05558	–0.112	0.36763	–0.152	0.24968
	HLA-DPA1	0.0151	0.70767	0.0256	0.55113	–0.064	0.60512	–0.103	0.43795
	CD1C	0.0002	0.99583	0.0209	0.6258	–0.032	0.79705	–0.087	0.51437
	NRP1	0.0167	0.6784	0.0085	0.84359	–0.232	0.05912	–0.287	0.0277
	ITGAX	0.06	0.13662	0.0765	0.07423	–0.305	0.01237	–0.327	0.01168
	CD209	–0.009	0.81833	–0.007	0.86746	–0.217	0.07838	–0.232	0.07743
Th1 cells	TBX21	0.1012	0.01201	0.1262	0.00315	–0.092	0.45583	–0.126	0.34113
	STAT4	0.0819	0.04208	0.1013	0.01785	–0.065	0.59861	–0.149	0.26012
	STAT1	0.0637	0.11403	0.0693	0.10557	–0.058	0.64179	–0.083	0.53017
	IFNG	0.0753	0.06176	0.0908	0.03383	–0.158	0.20114	–0.19	0.14913
	TNF	0.068	0.09176	0.1024	0.01664	–0.136	0.27332	–0.152	0.25042
Th2 cells	GATA3	–0.184	4.72E-06	–0.177	3.32E-05	0.227	0.06506	0.2474	0.05909
	STAT6	–0.043	0.29169	–0.03	0.47886	0.14	0.25811	0.1025	0.43873
	STAT5A	–0.073	0.07053	–0.058	0.17648	–0.212	0.08473	–0.263	0.04417
	IL13	0.0896	0.02615	0.098	0.02204	0.022	0.86036	0.0119	0.92879
Tfh cells	BCL6	–0.17	2.21E-05	–0.163	0.00013	–0.063	0.60962	0.0324	0.80724
	IL21	0.0302	0.45494	0.0418	0.33013	0.144	0.24355	0.093	0.48371
Th17 cells	STAT3	–0.008	0.8475	0.009	0.83457	–0.018	0.88411	–2E-04	0.99912
	IL17A	0.0249	0.53704	0.0591	0.16767	0.143	0.24853	0.1265	0.33956
Treg	FOXP3	0.1595	7.15E-05	0.1863	1.21E-05	–0.119	0.33485	–0.153	0.24548
	CCR8	0.1429	0.00038	0.1647	0.00011	–0.276	0.02383	–0.314	0.01581
	STAT5B	–0.035	0.39027	–0.027	0.53078	–0.132	0.28632	–0.166	0.20791
	TGFB1	–0.054	0.17878	–0.075	0.08017	–0.284	0.02011	–0.305	0.01931

Table S3 (*continued*)

https://dx.doi.org/10.21037/atm-21-6611

Table S3 (*continued*)

Description	Gene markers	Luminal Breast Cancer				Her-2 positive Breast Cancer			
		None		Purity		None		Purity	
		COR	P	COR	P	COR	P	COR	P
T cell exhaustion	PDCD1	0.1188	0.00314	0.1478	0.00053	–0.156	0.20765	–0.23	0.08006
	CTLA4	0.1227	0.00228	0.154	0.0003	–0.078	0.52941	–0.103	0.43768
	LAG3	0.1115	0.00559	0.1277	0.0028	0.01	0.93839	–0.009	0.94676
	HAVCR2	0.0488	0.22686	0.0604	0.15884	–0.337	0.00553	–0.35	0.00691
	GZMB	0.0946	0.01881	0.1248	0.00348	–0.014	0.91285	–0.061	0.646

COR, Correlation coefficient; Her-2, human epidermal growth factor receptor 2; CD, cluster of differentiation; TAM, tumor-associated macrophage; Th, T-helper; Tfh, follicular helper T; Treg, regulatory cells; FCRL2, Fc receptor like 2; MS4A1, membrane spanning 4-domains A1; FCGR3B, Fc gamma receptor IIIb; CEACAM, CEA cell adhesion molecule; SIGLEC5, sialic acid binding Ig like lectin 5; FPR1, formyl peptide receptor 1; CSF3R, colony stimulating factor 3 receptor; S100A12, S100 calcium binding protein A12; ITGAM, integrin subunit alpha M; CCR, C-C motif chemokine receptor; KIR2DL, killer cell immunoglobulin like receptor, two Ig domains and long cytoplasmic tail; KIR3DL, killer cell immunoglobulin-like receptor with three domains and long cytoplasmic tail; KIR2DS4, killer cell immunoglobulin like receptor, two Ig domains and short cytoplasmic tail 4; NCR1, natural cytotoxicity triggering receptor 1; C3AR1, complement C3a receptor 1; CSF1R, colony stimulating factor 1 receptor; CCL2, C-C motif chemokine ligand 2; IL, interleukin; NOS2, nitric oxide synthase 2; IRF5, interferon regulatory factor 5; PTGS2, prostaglandin-endoperoxide synthase 2; VSIG4, V-set and immunoglobulin domain containing 4; MS4A4A, membrane spanning 4-domains A4A; HLA-DPB1, major histocompatibility complex, class II, DP beta 1; HLA-DQB1, major histocompatibility complex, class II, DQ beta 1; HLA-DRA, major histocompatibility complex, class II, DR alpha; HLA-DPA1, major histocompatibility complex, class II, DP alpha 1; CD1C, CD1c molecule; NRP1, neuropilin 1; ITGAX, integrin subunit alpha X; TBX21, T-box transcription factor 21; STAT, signal transducer and activator of transcription; IFNG, interferon gamma; TNF, tumor necrosis factor; GATA3, GATA binding protein 3; BCL6, B cell leukemia transcription repressor; FOXP3, forkhead box P3; TGFB1, transforming growth factor beta 1; PDCD1, programmed cell death 1; CTLA4, cytotoxic T-lymphocyte associated protein 4; LAG3, lymphocyte activating 3; HAVCR2, hepatitis A virus cellular receptor 2; GZMB, granzyme B.

https://dx.doi.org/10.21037/atm-21-6611

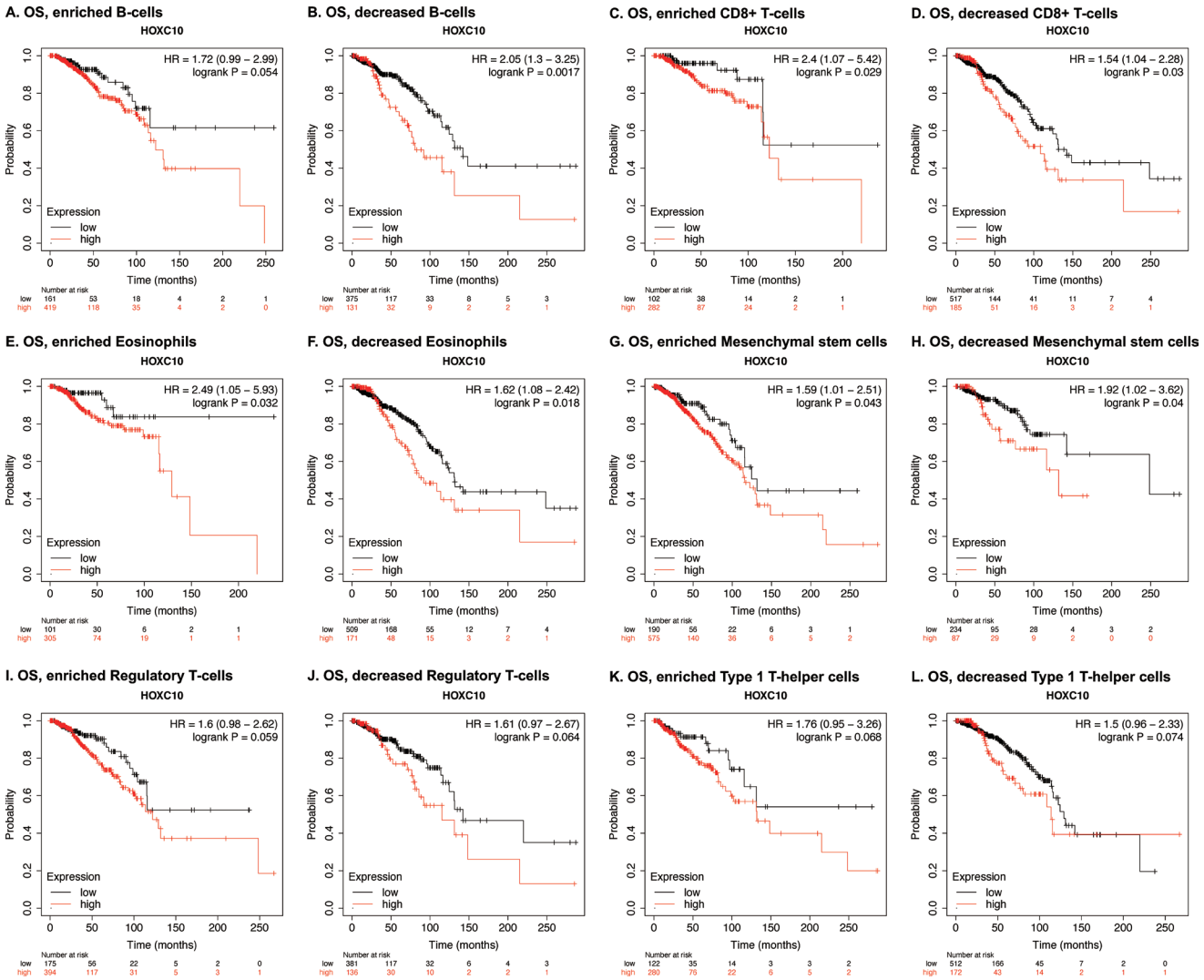

Figure S6 The correlations between *HOXC10* expression and the OS of breast cancer patients based on the different subgroups of immune cells in the Kaplan-Meier plotter database. (A) enriched B cells; (B) decreased B cells; (C) enriched $CD8^+$ T cells; (D) decreased $CD8^+$ T cells; (E) enriched eosinophils; (F) decreased eosinophils; (G) enriched mesenchymal stem cells; (H) decreased mesenchymal stem cells; (I) enriched Tregs (J) decreased Tregs; (K) enriched Type 1 T-helper cells; and (L) decreased Type 1 T-helper cells. OS, overall survival; CD, cluster of differentiation; Tregs, regulatory cells.

https://dx.doi.org/10.21037/atm-21-6611

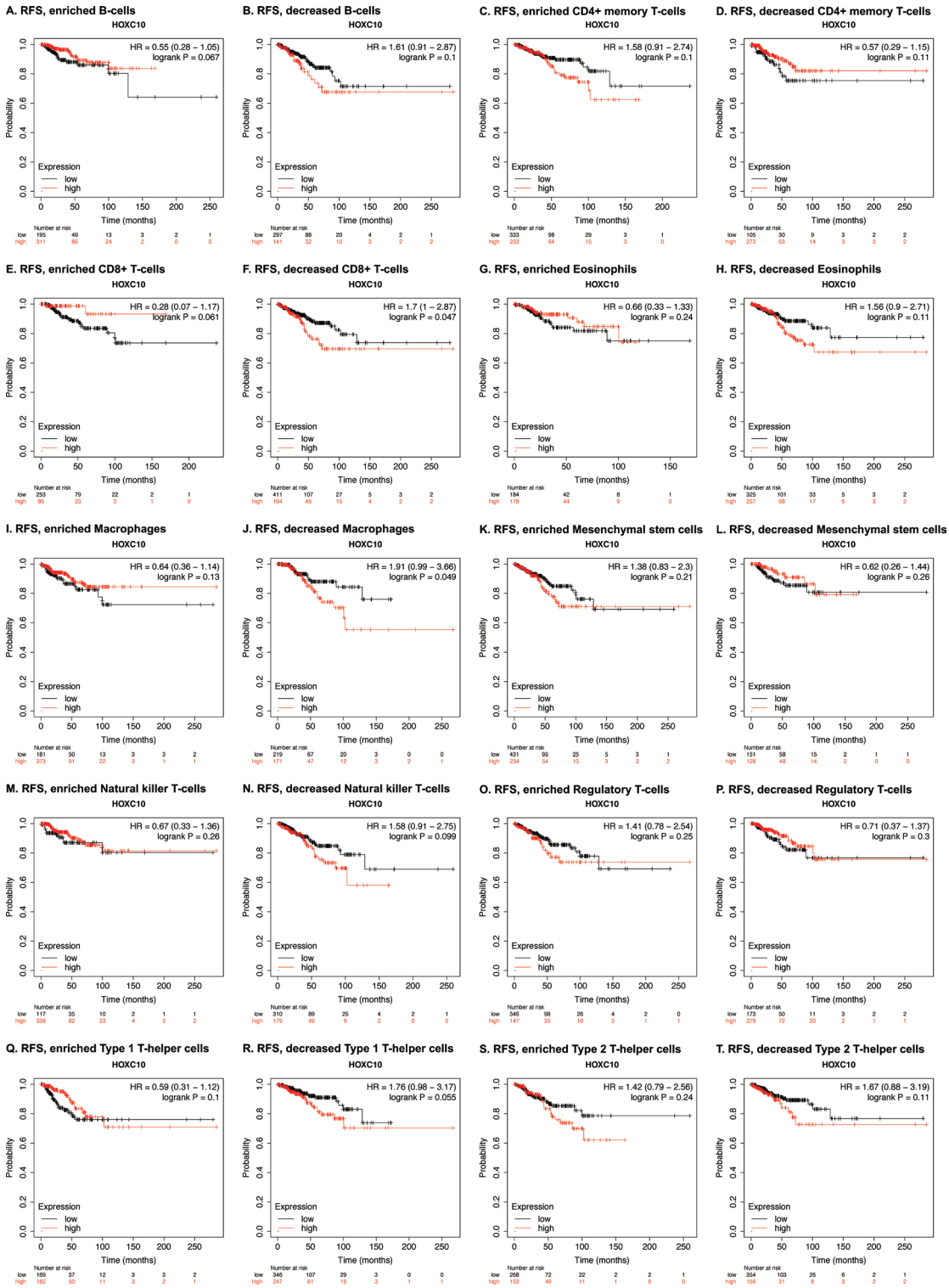

Figure S7 The interaction between *HOXC10* expression and the RFS of breast cancer patients based on the different subgroups of immune cells in the Kaplan-Meier plotter database. (A) enriched B cells; (B) decreased B cells; (C) enriched $CD4^+$ memory T cells; (D) decreased $CD4^+$ memory T cells; (E) enriched $CD8^+$ T cells; (F) decreased $CD8^+$ T cells; (G) enriched eosinophils; (H) decreased eosinophils; (I) enriched macrophages; (J) decreased macrophages; (K) enriched mesenchymal stem cells; (L) decreased mesenchymal stem cells; (M) enriched NK cells; (N) decreased NK cells; (O) enriched Tregs; (P) decreased Tregs; (Q) enriched Th1 cells; (R) decreased Th1 cells; (S) enriched Th2 cells; and (T) decreased Th2 cells. RFS, relapse-free survival; CD, cluster of differentiation; NK, natural killer; Tregs, regulatory cells; Th, T-helper.

https://dx.doi.org/10.21037/atm-21-6611